

Dynamical Reversibility and A New Theory of Causal Emergence

Jiang Zhang^{1,2*}, Ruyi Tao^{1,2}, Keng Hou Leong^{2,3},
Mingzhe Yang^{1,2}, Bing Yuan²

¹School of Systems Science, Beijing Normal University, No.19
Xinjiekouwai Street, Beijing, 100876, China.

²Swarma Research, Beijing, 100085, China.

³Tsinghua-Berkeley Shenzhen Institute, Tsinghua Shenzhen International
Graduate School, Tsinghua University, Shenzhen, 518055, China.

*Corresponding author(s). E-mail(s): zhangjiang@bnu.edu.cn;

Abstract

The theory of causal emergence based on effective information(EI) suggests that complex systems may exhibit a phenomenon called causal emergence(CE), where the macro-dynamics demonstrate a stronger causal effect than the micro-dynamics. However, a challenge in this theory is the dependence on the method used to coarse-grain the system. In this paper, we introduce a fresh concept of approximate dynamical reversibility and establish a novel framework for CE based on this and singular value decomposition. Our research not only reveals a strong correlation between the proximity of a Markov chain being dynamically reversible and EI in assessing causal effects across various scenarios but also demonstrates that EI is constrained by the logarithm of the approximate dynamical reversibility. Leveraging this concept, we present an innovative approach to quantifying CE that is agnostic to specific coarse-graining techniques and effectively captures the inherent characteristics of Markov dynamics. Through empirical evaluations on examples of boolean networks, cellular automata, and complex networks, we validate our refined CE definition.

Keywords: Dynamical Reversibility, Causal Emergence, Effective Information, Singular Value Decomposition, Markov Chain

1 Introduction

We live in a world surrounded by a multitude of complex systems. These systems engage in time-irreversible stochastic dynamics, leading to entropy production and disorder accumulation [1]. Despite this, there exists a belief that beneath the disorder in complex systems lie profound patterns and regularities [2, 3]. Consequently, researchers endeavor to derive causal laws from these dynamic systems at a macroscopic scale, while disregarding detailed micro-level information as appropriate [4–6]. Ultimately, the goal is to develop an effective theory or model capable of elucidating the causality of complex systems at a macroscopic level.

Such idea can be captured by the theoretical framework known as causal emergence(CE) proposed by Hoel et al. [5–7]. This framework builds upon an information-theoretic measure called Effective Information (EI) [8], which quantifies the causal influence between successive states within a Markov dynamical system. Through illustrative examples, they demonstrate that a coarse-grained Markov dynamics, when measured by EI at the macro-level, can exhibit stronger causal power than at the micro-level. Nevertheless, one of the foremost challenges is that the manifestation of CE relies on the specific manner in which we coarse-grain the system. Different coarse-graining methods may yield entirely disparate outcomes for CE [7]. While this issue can be mitigated by maximizing EI [5, 9, 10] or employing other indicators of CE that are independent of coarse-graining [11], the computational complexity and the question of solution uniqueness remain open challenges [7, 10]. Is it possible to construct a more robust theory of CE that is independent of the coarse-graining method?

Although Rosas et al. [11] proposed a new framework for CE based on partial information decomposition theory [12], which does not require a predefined coarse-graining strategy, it still involves iterating through all variable combinations to compare synergistic information, resulting in significant computational complexity. Rosas et al. also proposed an approximate method to mitigate the complexity [11], but it requires a pre-defined macro-variable. In addition, Barnett and Seth [13] introduced a novel framework for quantifying emergence based on the concept of dynamical independence. If the micro-dynamics are unrelated to the prediction of macro-dynamics, the complex system is considered to exhibit emergent macroscopic processes. However, this framework has only been applied to linear systems to date. Both of these methods for quantifying emergence are established on mutual information derived from data, leading to outcomes that are influenced by data distribution. Consequently, these results may not exclusively capture the “causal” or the dynamic essence of the system.

This paper endeavors to construct a theory based on an intriguing and slightly different concept: the reversibility of dynamics. In fact, there is deep connection between causality and the reversibility [14–19]. When we say that event A causes event B, we mean that not only does B occur when A occurs, but also when A does not occur, B must not occur (Counterfactual). This implies that we can not only infer B from A, but also infer the occurrence of A based on the occurrence of B. Consequently, the underlying dynamical process that determines how A causally affects B is reversible [14, 20]. This point is further supported by examples found in references [5, 6], where EI, as a measure of causality, is maximized when the underlying dynamics are reversible. Therefore, we can re-frame the theory of CE as an endeavor

to obtain a reversible macro-level dynamics by appropriately disregarding micro-level information.

This paper commences by introducing an indicator designed to measure the proximity of a Markov chain to be dynamically reversible, utilizing the singular values of its transitional probability matrix (TPM). Subsequently, it provides several formal definitions and mathematical theorems to establish the validity of the indicator and its close association with EI. Additionally, a novel definition for CE based on the approximate dynamical reversibility is introduced, followed by the validation of this definition and a demonstration of its equivalence to, and distinctions from, EI-based causal emergence using multiple examples including boolean networks, cellular automata, and complex networks. Finally, a more streamlined and potent coarse-graining method for general Markov chains, employing the singular value decomposition (SVD) of the TPM, is proposed.

2 Theories

2.1 Effective information and causal emergence

First, we will briefly introduce Hoel et al.’s theory of Causal Emergence (CE), which is grounded in the information-theoretic measure known as Effective Information (EI). This measure was initially introduced in [8] and has since been employed to quantify causal emergence in the work of Hoel et al. in [5]. For a given Markov chain χ with a discrete state space \mathcal{S} and the transitional probability matrix (TPM) P , EI is defined as:

$$EI \equiv I(X_{t+1}; X_t | do(X_t \sim U)), \quad (1)$$

where $X_t, X_{t+1}, \forall t \geq 0$ represent the state variables defined on \mathcal{S} at time step t and $t + 1$, respectively. The do-operator, denoted as $do(X_t \sim U)$, embodies Pearl’s intervention concept as outlined in [21]. This intervention enforces X_t to adhere to a uniform (maximum entropy) distribution on \mathcal{S} , specifically $Pr(X_t = i) = 1/N$, where $i \in \mathcal{S}$ and N represents the total number of states in \mathcal{S} . Given that $Pr(X_{t+1} = j) = \sum_{i \in \mathcal{S}} p_{ij} \cdot Pr(X_t = i)$, the do-operator indirectly influences $Pr(X_{t+1})$ as well. Here, p_{ij} denotes the element at the intersection of the i th row and the j th column in matrix P , indicating the transition probability from state i to state j . Consequently, the EI metric quantifies the mutual information between X_t and X_{t+1} subsequent to this intervention, thereby measuring the strength of the causal influence exerted by X_t on X_{t+1} .

An essential point to note in this definition is that while the *do* operator is employed in Eq. 1, it is essentially a symbolic operation; there is no actual physical intervention on X_t required. The rationale behind using the *do* operator is to ensure that the EI metric purely captures the characteristics of the underlying dynamics, specifically the TPM (P), while remaining unaffected by the distribution of X_t [7]. This point can be

more clear by showing another equivalent form of EI [5]:

$$EI = \frac{1}{N} \sum_{i=1}^N \sum_{j=1}^N p_{ij} \log \frac{p_{ij}}{\frac{\sum_{k=1}^N p_{kj}}{N}} = \frac{1}{N} \sum_{i=1}^N (P_i \cdot \log P_i - P_i \cdot \log \bar{P}) = \frac{1}{N} \sum_{i=1}^N D_{KL}(P_i || \bar{P}), \quad (2)$$

where P_i is the row vector of $P = (P_1, P_2, \dots, P_N)^T$, $D_{KL}(\cdot || \cdot)$ is the KL-divergence between two probability distributions, and $\bar{P} = \frac{1}{N} \sum_i P_i$ is the average vector of all the N row vectors of the TPM. Thus, EI measures the average KL-divergence between any P_i and their average \bar{P} . To be noted that, this form of EI is the generalized Jensen-Shannon divergence as mentioned in [22]. All the logarithms in Eq.3 is base on 2.

Furthermore, EI can be decomposed into two terms [5]:

$$EI = \frac{1}{N} \sum_{i=1}^N P_i \cdot \log P_i - \frac{1}{N} \sum_{i=1}^N P_i \cdot \log \bar{P} = \underbrace{-\bar{H}(P_i)}_{\text{determinism}} + \underbrace{H(\bar{P})}_{-\text{degeneracy}}, \quad (3)$$

the first term is determinism $-\bar{H}(P_i) \equiv \frac{1}{N} \sum_{i=1}^N P_i \cdot \log P_i$ which measures how the current state can deterministically(sufficiently) influences the state in next time step, and the second term is non-degeneracy $H(\bar{P}) \equiv -\sum_{j=1}^N \bar{P}_j \log \bar{P}_j$ which measures how exactly we can infer(necessarily) the state in previous time step from the current state. In their original definition in [5], both the determinism and the degeneracy are added $\log N$ to guarantee them to be positive. This decomposition reveals why EI can measure the strength of causal effect of a Markov chain and the connections with the reversibility of dynamics because the determinism can be understood as a kind of sufficiency and the degeneracy is a kind of necessity [7, 20].

This point can be more clear by the examples shown in Figure 1, where four cases of TPMs are shown and the EI values and their normalized forms $eff \equiv EI / \log_2 N$ are also demonstrated below. It is not difficult to observe that as the TPM is closed to a invertible matrix(a permutation matrix, see Theorem 1 in Appendix A.2.1), EI is larger.

Causal emergence occurs when the coarse-grained TPM possessing larger EI than the original TPM. As shown in the example in Figure 1(d), which is the coarse-grained TPM of the example in Figure 1(c). And the degree of CE can be calculated as the difference between the EI s:

$$CE = EI(P') - EI(P), \quad (4)$$

where, P' is the coarse-grained TPM of P . In this example, the coarse-graining is implemented by collapsing the first three rows and columns of the TPM in Figure 1(c) into one macro-state. Thereafter, $EI(P') = 1$ (or $eff = 1.0$) in (d) is clearly larger than $EI(P) = 0.81$ (or $eff = 0.41$) in (c), which manifests that the strength of cause-effect in macro-level (coarse-grained TPM in (d)) is larger than the micro-level (c), thus, causal emergence occurs, and the degree of CE is $1 - 0.81 = 0.19$.

	(a)		(b)
TPM:	$\begin{pmatrix} 1 & 0 & 0 & 0 \\ 0 & 0 & 0.9 & 0.1 \\ 0 & 0.9 & 0.1 & 0 \\ 0 & 0 & 0 & 1 \end{pmatrix}$		$\begin{pmatrix} 0.1 & 0.5 & 0.3 & 0.1 \\ 0.2 & 0.2 & 0.6 & 0 \\ 0 & 0.9 & 0 & 0.1 \\ 0.91 & 0 & 0.09 & 0 \end{pmatrix}$
Quantity:	$EI = 1.76$	$\Gamma = 3.81$	$EI = 0.77$ $\Gamma = 2.66$
Normalized:	$eff \equiv \frac{EI}{\log_2 N}$ $= 0.88$	$\gamma \equiv \frac{\Gamma}{N}$ $= 0.95$	$eff = 0.39$ $\gamma = 0.66$
	(c)		(d)
TPM:	$\begin{pmatrix} 1/3 & 1/3 & 1/3 & 0 \\ 1/3 & 1/3 & 1/3 & 0 \\ 1/3 & 1/3 & 1/3 & 0 \\ 0 & 0 & 0 & 1 \end{pmatrix}$	Coarse-graining \longrightarrow	$\begin{pmatrix} 1/3 & 1/3 & 1/3 & 0 \\ 1/3 & 1 & 1/3 & 0 \\ 1/3 & 1/3 & 1/3 & 0 \\ 0 & 0 & 0 & 1 \end{pmatrix}$
Quantity:	$EI = 0.81$	$\Gamma = 2$	$EI = 1$ $\Gamma = 2$
Normalized:	$eff = 0.41$	$\gamma = 0.5$	$eff = 1$ $\gamma = 1$

Fig. 1 Examples of transitional probability matrices (TPMs) used in different Markov chains, along with measures of effective information (EI and normalized one eff) for causality, and the measure of Γ_α (and normalized one γ_α by setting $\alpha = 1$) for approximate reversibility of dynamics.

2.2 Dynamical reversibility

Second, we will introduce the conception of dynamical reversibility for a Markov chain, and propose a quantitative indicator to measure the proximity for a general Markov chain to be dynamically reversible.

2.2.1 Definitions and Properties

Definition 1. For a given markov chain χ and the corresponding TPM P , if P simultaneously satisfy: 1. P is an invertible matrix, that is, there exists a matrix P^{-1} , such that $P \cdot P^{-1} = I$; and 2. P^{-1} is also an effective TPM of another Markov chain χ^{-1} , then χ and P can be called dynamically reversible.

It is important to clarify that in this context, a dynamically reversible Markov chain differs from the commonly used term “time reversible” Markov chain [18, 23],

as dynamical reversibility necessitates the ability of P to be reversibly applied to each individual state, whereas the latter focuses on the reversibility of state space distributions. Actually, we can prove that the former implies the latter (Proposition 3 in Appendix A.2.1).

Further, the following theorem states that all the Markov chains satisfying the two conditions mentioned in Definition 1 are permutation matrices.

Theorem 1. *For a given markov chain χ and the corresponding TPM P , if P is dynamical reversible as defined in Definition 1, if and only if P is a permutation matrix.*

Proof. The proof is referred to Appendix A.2. □

However, permutation matrices are rare in the whole class of all possible TPMs. That means, in the case of a general TPM, it is not inherently reversible. Hence, an indicator that can quantify the proximity for a general TPM being reversible is required.

It seems that the rank r of P can be this indicator because if and only if $r < N$, the matrix P is irreversible, and P is more degenerate the less is r . However, a non-degenerate(full rank) P is not always dynamically reversible because despite the inverse P^{-1} exists, it may not be an effective TPM, which means the normalization condition(the one-norm of the i th vector P_i in P should be one: $\|P_i\|_1 = 1$) is not satisfied. While, according to Theorem 1, TPMs must be permutation matrices to be dynamically reversible. Thus, the matrices being close to permutation matrices should be more reversible. One of an important observation is that all the row vectors in a permutation matrix are one-hot vectors(the vectors with only one element is 1, all other elements are zero). This characteristic can be captured by the Frobenius norm of P , $\|P\|_F$. Actually, if and only if the row vectors in P are one-hot vectors, $\|P\|_F$ is maximized (see Proposition 4 in Appendix A.2.1).

Therefore, the indicator that characterizes the approximate dynamical reversibility should be a kind of mixture of the rank and the Frobenius norm. While, the rank of a matrix P can also be written as:

$$r = \sum_{i=1}^N \sigma_i^0, \quad (5)$$

where $\sigma_i \geq 0$ is the i th singular value of P . Furthermore, according to Proposition 4 in Appendix A.2.1, the Frobenius norm can be written as:

$$\|P\|_F^2 = \sum_{i=1}^N \sigma_i^2, \quad (6)$$

which is also the sum of the squares of singular values. Both the rank and the Frobenius norm are connected with the singular values of P .

Formally, the approximate dynamical reversibility of P can be formalized by the following definition:

Definition 2. Suppose the transitional probability matrix (TPM) is P for a markov chain χ , and its singular values are $(\sigma_1 \geq \sigma_2 \geq \dots \geq \sigma_N \geq 0)$, then the α ordered approximate dynamical reversibility of P is defined as:

$$\Gamma_\alpha \equiv \sum_i^N \sigma_i^\alpha, \quad (7)$$

where $\alpha \in (0, 2)$ is a parameter.

Actually, Γ_α is the Schatten norm of P : $\Gamma_\alpha = \|P\|_\alpha^\alpha$ when $\alpha \geq 1$ (it is also called nuclear norm when $\alpha = 1$), while it is quasinorm when $0 < \alpha < 1$ [24–27].

This definition is reasonable to characterize the approximate dynamical reversibility because the exact dynamical reversibility can be obtained by maximizing Γ_α as mentioned by the following Theorem:

Theorem 2. The maximum of Γ_α is N for any $\alpha \in (0, 2)$, and it can be achieved if and only if P is a permutation matrix.

Proof. The proof can be referred by Appendix A.2.2. \square

Further, Γ_α is lower bounded by $\|P\|_F^\alpha$ according to Proposition 6, and this lower bound can be increased if the dynamics P is more deterministic (more one-hot row vectors in P) according to Proposition 7. For fully deterministic TPMs (all row vectors are one-hot vectors), Γ_α can be further increased as the number of orthogonal vectors become larger as claimed by Proposition 8. In general, when P is close to a permutation matrix, Γ_α approaches its maximum. These propositions guarantee that Γ_α is a reasonable indicator to measure the approximate dynamical reversibility for any given P . All the mathematical proves are given in Appendix A.2.2.

2.2.2 Determinism and degeneracy

To be noticed that by adjusting parameter $\alpha \in (0, 2)$, we can make Γ_α more reflective of P 's **determinism** or **degeneracy**. When $\alpha \rightarrow 0$, Γ_α converges to the rank of P , which resembles the non-degeneracy term in the definition of EI (Equation 3) because r decreases as P is more and more degenerate. However, α is not allowed to take exact 0 in Definition 2 because $rank(P)$ is not a continuous function of P , and maximizing $rank(P)$ can not lead to permutation matrices.

Similarly, Γ_α converges to $\|P\|_F^2$ when $\alpha \rightarrow 2$, but α is not allowed to take exact 2 in Definition 2 because the maximization of $\Gamma_{\alpha=2}$ does not imply P being reversible. $\|P\|_F$ is comparable with the determinism term in the definition of EI (Equation 3) because when there are more and more one-hot row vectors in P , the maximum transitional probability in P become larger and larger which means the underlying dynamics becomes more deterministic.

In practice we always take $\alpha = 1$ to balance the propensity of Γ_α for measuring determinism and degeneracy, and $\Gamma_{\alpha=1}$ is called nuclear norm which has many potential practices [27, 28]. When $\alpha < 1$ the measure Γ_α quantifies more on the non-degeneracy of P . In literatures, $\Gamma_{\alpha \leq 1}$ is always utilized as an approximation of the rank function [29, 30]. While, the measure Γ_α characterizes more on the determinism of P when $\alpha > 1$.

Considering the importance of $\alpha = 1$, we major show the results on $\alpha = 1$, and we abbreviate Γ_1 as Γ in the following texts.

2.2.3 Normalization and Examples

Since Γ_α is size-dependent, we need to normalize them by dividing the size of P

$$\gamma_\alpha = \frac{\Gamma_\alpha}{N}, \quad (8)$$

to characterize the size-independent approximate dynamical reversibility such that the comparisons between Markov chains with different sizes are more reasonable. It can be proved that γ_α is always smaller than 1 as a derived result of Theorem 2.

In Figure 1, we show Γ_α s and the normalized ones, γ_α s, on the four examples by setting $\alpha = 1$. Γ varies from 2 (case c, d) to 3.81 (case a), and $\gamma = \Gamma/N$ varies from 0.5 (case c) to 1 (case d) in Figure 1. It is clear that γ is larger if the TPM is closed to a reversible matrix. And the correlation between γ and eff can be observed in these examples.

2.3 Connections between Γ_α and EI

On one side, EI characterizes the strength of causal effect of a Markov chain; on the other side, Γ_α can quantitatively capture the approximate dynamical reversibility of the Markov chain. We have claimed that the causality and reversibility are deeply connected in the introduction, thus, we will discuss the connections between EI and Γ_α in this sub-section.

First, we found that EI and $\log \Gamma_\alpha$ share the same minimum and maximum as mentioned in the following theorem.

Theorem 3. *For any TPM P and $\alpha \in (0, 1)$, both the logarithm of Γ_α and EI share identical minimum value of 0 and one common minimum point at $P = \frac{1}{N} \mathbb{1}_{N \times N}$. They also exhibit the same maximum value of $\log N$ with maximum points corresponding to P being a permutation matrix.*

Proof. The proof can be referred to Appendix A.3. □

Thus, $\log \Gamma_\alpha$ and EI can reach their maximal values $\log N$ when P is reversible (permutation matrix). They also achieve their minimal values (0) when $P_i = \mathbb{1}/N, \forall i \in [1, N]$. However, we can prove that $\mathbb{1}/N$ is not the unique minimum point of EI , any TPM with $P_i = P_j$ for any $i, j \in [1, N]$ can make $EI = 0$ (see Proposition 1 and Corollary 1 in Appendix A.1).

Second, EI is upper and lower bounded by a linear term of $\log \Gamma_\alpha$. This point can be formally stated as the following theorems.

Theorem 4. *For any TPM P , its effective information EI is upper bounded by $\frac{2}{\alpha} \log \Gamma_\alpha$, and lower bounded by $\log \Gamma_\alpha - \log N$.*

Proof. The proof can be referred to Appendix A.3. □

Therefore, we have the following inequality:

$$\log \Gamma_\alpha - \log N \leq EI \leq \frac{2}{\alpha} \log \Gamma_\alpha. \quad (9)$$

Actually, a tighter upper bound for EI , $EI \leq \log \Gamma_\alpha$, is found empirically as the numeric results shown in the next section. We also found that EI and Γ_α always positively correlated in many cases. Therefore, we propose an approximate relationship exists:

$$EI \sim \log \Gamma_\alpha. \quad (10)$$

2.4 A new quantification for causal emergence

One of the major contribution of this paper is a new quantification for causal emergence based on dynamical reversibility and singular values, and this quantification is independent on any selection of coarse-graining method. Because Γ_α is the summation of the α powers of the singular values of P , removing zero or approximate zero singular values does not change Γ_α . This is the basic idea behind our quantification for CE.

First, two new definitions about causal emergence are given.

Definition 3. For a given markov chain χ with TPM P , if $r \equiv \text{rank}(P) < N$ then **clear causal emergence** occurs in this system. And the degree of CE is

$$\Delta\Gamma_\alpha = \Gamma_\alpha \cdot (1/r - 1/N). \quad (11)$$

Definition 4. For a given markov chain χ with TPM P , suppose its singular values are $\sigma_1 \geq \sigma_2 \geq \dots \geq \sigma_N \geq 0$. For a given real value $\epsilon \in [0, \sigma_1]$, if there is an integer $i \in [1, N)$ such that $\sigma_i > \epsilon$, then there is **vague causal emergence** with the level of vagueness ϵ occurred in the system. And the degree of CE is:

$$\Delta\Gamma_\alpha(\epsilon) = \frac{\sum_{i=1}^{r_\epsilon} \sigma_i^\alpha}{r_\epsilon} - \frac{\sum_{i=1}^N \sigma_i^\alpha}{N}, \quad (12)$$

where $r_\epsilon = \max\{i | \sigma_i > \epsilon\}$

These definitions are independent of any coarse-graining method. As a result, it represents an intrinsic and objective property of Markov dynamics. Thus, the occurrences of both clear and vague CE, as well as the extent of such emergence, can be objectively quantified.

It is not difficult to see that clear CE is a special case of vague CE when $\epsilon = 0$, and it has theoretical values particularly when the singular values can be solved analytically. Furthermore, the judgement on the occurrence of CE is independent on α because it relates only on the rank. As a result, the notion of clear CE is only determined by P and is parameter free.

While, in practice the threshold ϵ must be given because the singular values may approach 0 infinitely but P is full rank. ϵ can be selected according to the relatively

clear cut-offs in the spectrum of singular values (or the logarithm of singular values). If ϵ is very small (say $\epsilon < 10^{-10}$), we can also say CE occurs roughly.

As Proposition 9 claims, $\Delta\Gamma_\alpha(\epsilon) \in [0, N - 1]$ for any $\epsilon \geq 0$, and CE occurs if and only if $\Delta\Gamma_\alpha(\epsilon) > 0$ according to Proposition 10. The propositions and the proves can be found in Appendix A.3.1.

3 Results

In this section, we will show the numeric results on the comparison between EI and Γ_α , the quantification of CE under the new framework. A new method of coarse-graining based on SVD is proposed to compare the results derived from EI. In this section, we use Γ to abbreviate $\Gamma_{\alpha=1}$ if there is no extra declarations.

3.1 Comparisons of EI and Γ

3.1.1 Similarities

In section 2.3, we have derived that EI is upper and lower bounded by a linear term of $\log \Gamma_\alpha$ and we conjecture an approximate relationship: $EI \sim \log \Gamma_\alpha$ in theory. We will further verify these conclusions by numeric experiments in this section.

We compare Γ_α and EI on a variety of normalized TPMs generated by three different methods: 1) softening of permutation matrices; 2) softening of degenerate matrices; and 3) total random. The details of these generative models are in Appendix B. The results are shown in Figure 2.

As shown in Figure 2(a), (b) and (c), a positive correlation is observed on all these examples, and the approximate relationship $EI \sim \log \Gamma$ is confirmed for large $N \gg 1$. This relation is obviously observed in Figure 2(a) and (b), but degenerates to a nearly linear relation in Figure 2(b) since limited value region of Γ is covered. More results on different α can be referred to Appendix section B.1.

We also show the upper and lower bounds of EI by the red dashed lines in Figure 2(a) and (b). However, in Figure 2(c), the theoretical bounds lines are invisible because all the points are concentrated in a small region.

Empirically, a tighter upper bound of EI by $\log \Gamma_\alpha$ is found as the grey broken lines shown in Figure 2. Therefore, we conjecture a new relationship, $EI \leq \log \Gamma_\alpha$ holds, but the rigour proof left for future works.

We also obtain the analytic solution for EI and Γ on the simplest parameterized TPM with size $N = 2$ (see Appendix C), and we show the landscape how EI and Γ are dependent on the parameters p and q . It is clear that both EI and Γ obtain their maximum values on the anti-diagonal regions ($p = q = 0$ or $p = q = 1$, in this case, P is a permutation matrix). The differences between Figure 2(c) and (d) are apparent: 1) Γ has a peak value when $p \approx 1 - q$ but EI has not; 2) a broader region with $EI \approx 0$ is observed, while the region with $\Gamma \approx 1$ is much smaller; 3) an asymptotic transition from 0 to maximal $N = 2$ is observed for Γ , but not for EI .

Therefore, we conclude EI and Γ_α are highly correlated on various TPMs.

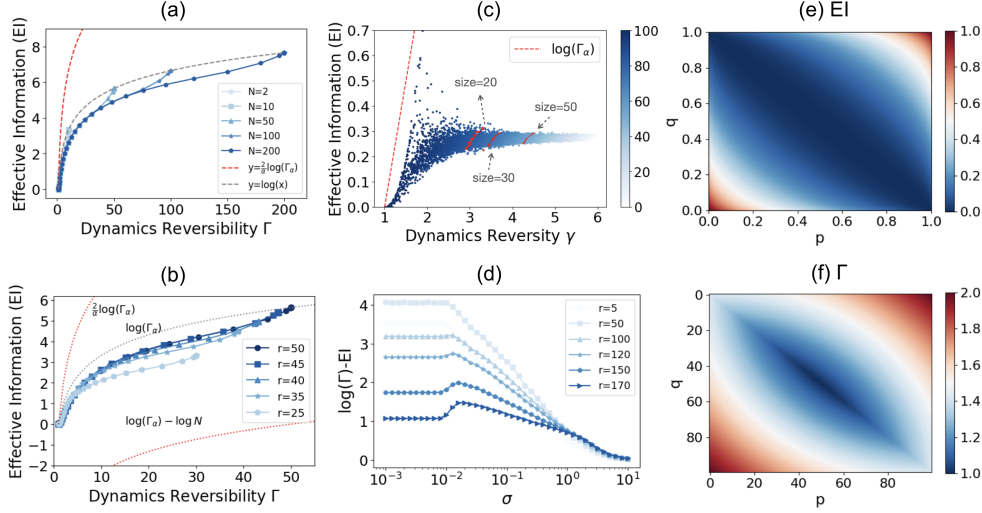


Fig. 2 Comparison between EI and $\Gamma_{\alpha=1}$ for various generated TPMs. (a) shows the approximate relationship $EI \sim \Gamma$ for randomly generated TPMs which are softening of permutation matrices, the theoretical and empirical upper bounds are also shown as dashed lines. The lower bound is omitted because it is size-variant. The method for softening is by adding a value y on each entry locating at the i th row and the j th column of the generated permutation matrix P , where $y = \frac{1}{\sqrt{2\pi}\sigma} \exp -\frac{(j-c_i)^2}{\sigma^2}$, and c_i is the position of the element with value one for the i row vector as a one-hot vector, σ is a parameter to control the intensity of the softening. Each curve is obtained by tuning up the magnitude of softening on a randomly generated permutation matrix with different sizes. (b) demonstrates the same relationship between EI and Γ for the TPMs which are generated by the similar softening method, but which are based on a variance of the $N \times N$ identity matrix. The variance is to change $N - r$ row vectors of identity matrix to the same one-hot vectors (with the value one as the first element), where r is the rank of the matrix, $N = 50$. And the number $N - r$ can be treated as a control of the degeneracy of the TPM. On this figure, all the upper bounds and lower bounds are shown as dashed lines. (c) shows the same relationship for the combination of randomly sampled normalized row vectors for various sizes ($N \in [2, 100]$). On each size, 100 such random matrices are sampled to get the scatter points. The scatter points for particular sizes $N = 20, 30, 50$ are rendered with red to show the nearly logarithmic relation between EI and Γ . The empirical upper bound is also shown as the dashed line. (d) demonstrates the dependence of the difference between EI and Γ ($\log \Gamma - EI$) on the softening magnitude σ for the matrices generated. The matrices are composed by r orthogonal one hot vectors as the base vectors, and $N - r$ one-hot vectors which are the linear combinations of the base vectors, and the coefficients are sampled by random real numbers uniformly distributed on $[0, 1]$. After the generation, we use the similar method to soften the one-hot vectors with the magnitude of σ . The size $N = 50$ is fixed in these experiments. (e) and (f) shows the density plots of EI (c) and Γ (d) with different parameters p and q computed for a parameterized simplest TPM: $P = \begin{pmatrix} p & 1-p \\ 1-q & q \end{pmatrix}$ with size 2×2

3.1.2 Differences

Although deep connections between EI and Γ_{α} have been found, differences between these two indicators exist.

Firstly, EI quantifies the distinctions between each row vector and the average row vector of P through KL-divergence as defined in Equation 2. Put differently, EI gauges the resemblances among the row vectors. Conversely, Γ_α assesses the dynamic reversibility, particularly as α approaches 0, which correlates with the linear interdependence among the row vectors. While the linear interdependence of row vectors suggests their similarity – meaning two identical row vectors are linearly dependent – the reverse is not necessarily true. Consequently, Γ_α not only captures the similarities among row vectors but also the proximity of P to a dynamically reversible matrix. In contrast, EI cannot accomplish this task.

This assertion can be validated through the following numerical experiments: we can create TPMs by blending linearly dependent row vectors with linearly independent row vectors, where the number of independent vectors, or the rank, is a controlled parameter. Initially, we generate r independent one-hot vectors, then soften these row vectors using the same method as described in Appendix section B.1, with the degree of softening determined by σ . Subsequently, we create additional row vectors by linearly combining these softened one-hot vectors with randomly chosen linear coefficients. We then quantify the disparity between Γ and EI , with the outcomes depicted in Figure 2(d).

It becomes evident that for small values of r , with increasing σ , the disparity between $\log \Gamma$ and EI diminishes, given that the linear dependency of P strengthens as vectors become more distinct. This underscores that linear dependency does not equate to similarity between row vectors. However, as the number of independent row vectors grows, if σ remains small, P converges towards a permutation matrix. Consequently, both EI and $\log \Gamma$ reach identical maximum values. This elucidates why a slight bump is noticeable when r is substantial.

Secondly, a significant distinction exists between EI and Γ_α even in scenarios where all row vectors are identical, resulting in $EI = 0$ while $\Gamma_\alpha = \|\bar{P}\|^\alpha \cdot N^{\alpha/2}$, a quantity that can vary with $\|\bar{P}\|$ (refer to Lemma 4, Appendix A.2). This discrepancy implies that Γ_α – as opposed to EI – can provide more comprehensive insights regarding the row vectors beyond their similarity to the average row vector.

3.2 Quantifying causal emergence

Examples for clear and vague CE are shown in this section. First, to show the validity of our new framework for CE, several Markov dynamics on boolean networks which have been proposed in Hoel et al.’s papers [5, 6] are selected to test our method, and compare with the results for CE derived from the method of EI.

Two examples of TPMs generated from the same boolean network model with identical node mechanism for clear emergence and vague emergence are shown in Figure 3(a-i), respectively. The TPM in Figure 3(d) is derived from the boolean network and its node-mechanism in Figure 3(a) and (b) directly. Their singular value spectra are shown in Figure 3(e) and (h), respectively.

There are only 4 non-zero singular values (Figure 3(e)) for the first example in (d), therefore, clear CE occurs, and the degree of CE is $\Delta\Gamma = 0.75$. This judgement for CE is the same as in ref [5].

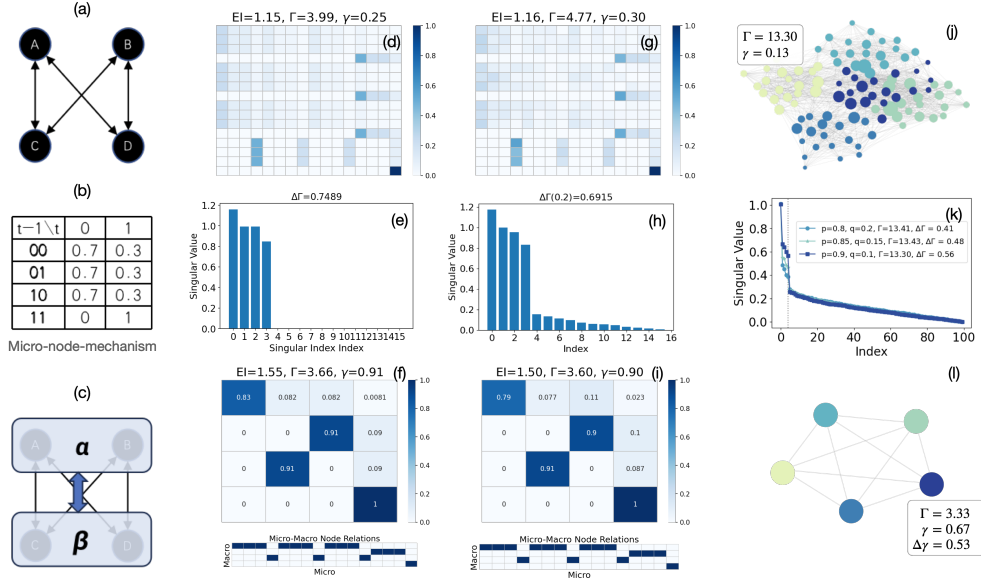


Fig. 3 Examples of clear and vague CE and their coarse-grained models based on SVD method for a boolean network and complex networks generated by the stochastic block models. (a) The original stochastic boolean network model, each node can only interact with its network neighbors; (b) Node dynamics in (a). Each row corresponds to the states combination of one node's all neighbors in previous time step, and each column is the probability that to take 0 or 1 of the node at current time step. (c) The coarse-grained boolean network of (a) which is extracted from the TPMs of (f) and (i). (d) The corresponding TPM of (a) and (b). (e) The singular value spectrum for (d). (g) A perturbed TPM from (d). (h) The singular value spectrum for (g). (f) and (i) are the reduced TPMs and the projection matrices (below) after the applications of our coarse-graining method on the original TPMs in (d) and (g), respectively. (j) is the original network sampled from the stochastic block model with $p = 0.9$ (the probability for inner community connections) and $q = 0.1$ (the probability for inter community connections). The edges are undirected and binary. The TPM is obtained by normalizing the adjacency matrix by dividing each node's degree. (k) The singular value spectrum of three samples of the stochastic block model network with different p and q . (l) is the reduced network of (j) by utilizing our coarse-graining method. The clusters of nodes identify the blocks correctly..

Vague CE can be shown on the TPM in Figure 3(g), which is derived from (d) by adding random Gaussian noise with strength ($std = 0.03$) on the TPM in (d). As a result, the singular spectrum is obtained as shown in Figure 3(h). We select $\epsilon = 0.2$ as the threshold such that only 4 large singular values are left. The degree of CE is $\Delta\Gamma(0.2) = 0.69$. The value of ϵ is selected according to the spectrum of singular values in Figure 3(h) where a clear cut-off at the index of 3 and $\epsilon = 0.2$ can be observed.

Figure 4(a-f) shows another example of clear CE on a more complex boolean network model from the reference of [5], where 6 nodes with the same node mechanism can be grouped into 3 super-nodes to show CE. The corresponding TPM of the original boolean network model is shown in Figure 4(c). The spectrum of the singular values is shown in Figure 4(d) where 8 non-zero values are found. The degree of this clear CE is $\Delta\Gamma = 2.23$. The same judgement of CE is obtained as in [5]. More examples on boolean networks in references [5] and [6] can be referred to Appendix Section E.1.

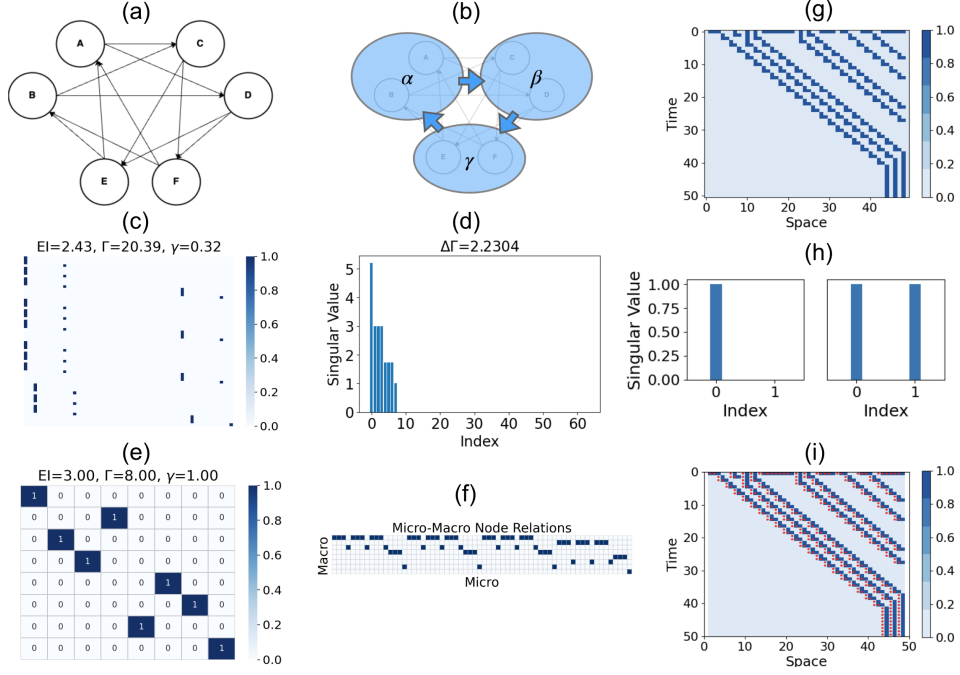


Fig. 4 Examples of clear causal emergence on a boolean network and a one-dimensional cellular automaton. (a) is the boolean network model with 6 nodes and 12 edges, the micro-mechanism can be referred to ref.[5]. (b) is the coarse-grained boolean network model according to the coarse-grained TPM of (e). (c) is the corresponding TPM of (a). (d) is the spectrum for the singular values of (c) with only 8 non-zero values. (e) is the coarse-graining of (c). (f) is the projection matrix from the macro-states to the micro-states obtained according to our coarse-graining method based on SVD. (g) is the evolution of the 40th elementary cellular automaton (the rule is $000 \rightarrow 0, 001 \rightarrow 0, 010 \rightarrow 1, 011 \rightarrow 0, 100 \rightarrow 1, 101 \rightarrow 0, 110 \rightarrow 0, 111 \rightarrow 0$). (h) shows the two spectra of the singular values for four distinct local TPMs of the same cellular automaton. (i) shows the local quantification of CE ($\Delta\Gamma$, the red dots) as well as the original evolution of the original automaton (the background).

The quantification for CE can be applied on complex networks (Figure 3(j-l)) and cellular automata (Figure 4(g-i)). The example of vague CE is shown for complex networks generated by stochastic block models(SBM) with three sets of parameters (inner or intra connection probabilities) on Figure 3(j-l). The TPMs are obtained by normalizing the adjacency matrix of the network by each node's degree. One of the exemplified network with 100 nodes and 5 blocks (communities) is shown in Figure 3(j) and its spectrum of singular values is shown in Figure 3(k) where a clear cut-off ($\epsilon = 0.3, r_\epsilon = 5$) can be observed at the horizontal coordinate as same as the number of blocks. We can ascertain that vague CE occurs in this network model with the degree of CE, $\Delta\Gamma(0.3) = 0.56$. Two more spectra of the networks generated by the SBM with the same size and the number of blocks but different parameters are shown in the same figure.

The definition on clear CE can be applied on cellular automata to discover its local emergent structures as shown in Figure 4(g-i). In this example, we quantify clear

CE for local TPMs of a cellular automaton (number 40 elementary one-dimensional cellular automaton). The local TPM is obtained by the local windows including each cell and its two neighbors. The possible spectra of singular values for these local TPMs are shown in Figure 4(h) where clear CE may or may not occur. Figure 4(i) shows the distributions of clear CEs ($\Delta\Gamma$) for all cells and time steps with the red dot markers. We also plot the original evolution of this automaton as the background.

3.3 Coarse-graining strategy based on SVD

Although clear or vague CE phenomena can be defined and quantified without coarse-graining, a simpler coarse-grained description for the original system is needed to compare with the results derived from EI. Therefore, we also provide a concise coarse-graining method based on the singular value decomposition of P to obtain a macro-level reduced TPM. The basic idea is to project the row vectors $P_i, \forall i \in [1, N]$ in P onto the sub-spaces spanned by the eigenvectors of $P \cdot P^T$ such that the major information of P is conserved, as well as Γ is kept unchanged.

The coarse-graining method contains five steps: 1) SVD decomposition for the TPM; 2) selecting an ϵ as the threshold to cut off the singular value spectrum, and to obtain r_ϵ as the number of retained states; 3) dimensionality reduction for all P_i in P by calculating $P \cdot V_{N \times r_\epsilon}$, where $V_{N \times r_\epsilon}$ is formed by the first r_ϵ eigenvectors of $P \cdot P^T$; 4) clustering all row vectors in $P \cdot V_{N \times r_\epsilon}$ into r_ϵ groups to obtain a projection matrix Φ ; and 5) obtain a new TPM by using Φ and P such that the total stationary flux is kept unchanged. The detailed information about this method and why it does work can be referred in Appendix D.

We test our method on all the examples shown in Figure 3 and 4. First, for the two TPMs generated according to the same boolean network model shown in Figure 3(d) and (g), their coarse TPMs are shown in Figure 3(f) and (i), respectively. The macro-level boolean network model (Figure 3(c)) can be read out from the TPMs and the projection matrix Φ . To be noticed, Γ s in the coarse TPMs are almost identical to the original ones, which means our method is Γ conservative in this case. We further test the examples of CE in the references [5, 6], and almost identical coarse TPMs can be obtained.

Second, the reduced TPM of the original one (Figure 4(a)) can be obtained by the same coarse-graining method as shown in Figure 4(e), and the projection matrix Φ is shown in (f). The coarse-grained boolean network can be read out from the reduced TPM and the projection matrix as shown in Figure 4(b). In this example, although Γ is reduced much (from $\Gamma = 20.39$ to $\Gamma = 8.0$) due to the information lose in coarse-graining, the normalized approximate dynamical reversibility is increased (from $\gamma = 0.32$ increase to $\gamma = 1.0$).

The same coarse-graining method can be also applied in complex networks generated by SBM. The reduced network with 5 nodes which is derived from the original network (Figure 3(j)) is shown in Figure 3(l). A relatively large decrease of Γ (from $\Gamma = 13.30$ to $\Gamma = 3.33$) and a large increase of γ (from $\gamma = 0.13$ to $\gamma = 0.67$) are also

observed in this example simultaneously. This indicates a large amount of information is lost during the coarse-graining, while a relatively more effective small network model with larger normalized approximate dynamical reversibility can be obtained.

3.4 Discussion and Conclusion

In summary, our investigation reveals that the Schatten norm, defined as the sum of the α powers of all singular values of a TPM, serves as a valuable indicator of the approximate dynamical reversibility within Markov dynamics. Both theoretical insights and empirical examinations substantiate a positive association, indicating a rough correspondence between the Effective Information (*EI*) metric and the logarithm of the measure Γ_α . Notably, it is crucial to distinguish between these two metrics. While Γ_α effectively quantifies the degeneracy of a TPM, particularly as $\alpha \rightarrow 0$, encompassing scenarios where all row vectors are nearly identical, *EI* solely characterizes the similarity between these row vectors and falls short in distinguishing degenerate yet dissimilar row vectors.

Expanding on the concept of Γ_α , we have introduced a novel CE theory that offers a more refined definition, capturing the intrinsic properties of a system regardless of the specific coarse-graining technique employed. Additionally, by leveraging Singular Value Decomposition (SVD) on a TPM, we have delineated a more efficient approach to system coarse-graining.

Furthermore, this research lays the groundwork for a potential connection between thermodynamics and Causal Emergence if we treat both coarse-graining and macro-dynamics (coarse-grained TPM) as thermodynamical processes. The onset of causation aligns with the rise of dynamical reversibility, a phenomenon that signifies a decrease in entropy production rate. Consequently, the fascination with emergent phenomena can be rationalized by the aspiration to attain macro-dynamics characterized by a diminished rate of entropy production. Nonetheless, this aspiration hinges on the extent of entropy production throughout the process of coarse-graining because of information loss during this process. Consequently, the dynamical balance between the rates of entropy production in macro-dynamics and coarse-graining necessitates additional scrutiny and investigation.

Nevertheless, there are limitations in this work. One of the major one is that all the aforementioned discussions have been centered around the state space, whereas an extension to the variable space would be more practical. However, it should be noted that the size of the state space grows exponentially with the number of variables, which poses a challenge.

Another defect in this study is the theoretical upper and lower bounds of *EI* by $\log \Gamma_\alpha$ should be further studied since tighter upper bound is observed empirically from numeric experiments but cannot be proved. More mathematical tools and methods should be developed to study this problem. As a result, further research is warranted to address these issues.

Acknowledgements. We wish to acknowledge all the members who participated in the “Causal Emergence Reading Group” organized by the Swarma Research and the “Swarma - Kaifeng” Workshop.

Support Information for Dynamics Reversibility and A New Theory of Causal Emergence

Appendix A Theorems and Proves

A.1 Propositions and proves for EI

We will layout the propositions about EI and give the proves for them in this subsection.

Proposition 1. *The EI can reach its minimum value 0 if and only if the row vectors of the probability transition matrix P are identical.*

Proof. The EI can be expressed as:

$$EI = \frac{1}{N} \sum_{i=1}^N D_{KL}(P_i || \bar{P}) = \frac{1}{N} \sum_{i=1}^N \sum_{j=1}^N p_{ij} \log \frac{N \cdot p_{ij}}{\sum_{k=1}^N p_{kj}}, \quad (\text{A1})$$

where, P_i is the i th row vector in P , and \log is the logarithm function with base 2. Without losing generality, suppose $p_{ij} > 0$, $p_{iN} > 0$, $\bar{p}_{\cdot j} > 0$, and $\bar{p}_{\cdot N} > 0$, then EI is differentiable on p_{ij} . By taking derivative, and using the normalization condition of probability distribution $\sum_{j=1}^N p_{ij} = 1$ for $1 \leq i \leq N$, we obtain that:

$$\frac{\partial EI}{\partial p_{ij}} = \log \left(\frac{p_{ij}}{p_{iN}} \right) - \log \left(\frac{\bar{p}_{\cdot j}}{\bar{p}_{\cdot N}} \right) \quad (\text{A2})$$

for $1 \leq i \leq N$ and $1 \leq j \leq N - 1$, where $\bar{p}_{\cdot j} = \frac{1}{N} \sum_{k=1}^N p_{kj}$ for $1 \leq j \leq N$. Therefore, Equation A2 is equal to 0 if and only if:

$$p_{ij} = p_{ij}^* = \bar{p}_{\cdot j} = \frac{1}{N} \sum_{k=1}^N p_{kj} \quad (\text{A3})$$

for any $1 \leq i, j \leq N$. That is to say, all the row vectors are identical: $P_i = P_j = \bar{P}$ for any $1 \leq i, j \leq N$. And the corresponding value of EI is:

$$EI_{min} = 0. \quad (\text{A4})$$

□

Therefore, EI can reach its minimum value 0 when all the row vectors are identical. For the special matrix $P = \frac{1}{N} \cdot \mathbf{1}$, EI also equals 0, however, it is not the unique minimum point. Actually, all the matrix with identical normalized probability vector can make $EI = 0$.

By further taking the second order derivative of EI , we can prove that EI is not a convex function.

Corollary 1. *The second order derivative of EI with respect to the distribution p_{st} with $1 \leq s \leq N$ and $1 \leq t \leq N - 1$ is:*

$$\frac{\partial^2 EI}{\partial p_{ij} \partial p_{st}} = \frac{1}{N} \cdot \left(\frac{\delta_{i,s} \delta_{j,t}}{p_{ij}} + \frac{\delta_{i,s}}{p_{iN}} - \frac{\delta_{j,t}}{N \cdot \bar{p}_{\cdot j}} - \frac{1}{N \cdot \bar{p}_{\cdot N}} \right), \quad (\text{A5})$$

and the $EI(\{p_{ij}\})$ is not a convex function.

Proof. By further taking the derivative of Equation A2 with respect to the distribution p_{st} with $1 \leq s \leq N$ and $1 \leq t \leq N - 1$, we obtain Equation A5.

When $i = s$, the second order derivative of EI is:

$$\begin{aligned} \frac{\partial^2 EI}{\partial p_{ij} \partial p_{it}} &= \frac{\delta_{j,t}}{N} \left(\frac{1}{p_{ij}} - \frac{1}{N \cdot \bar{p}_{\cdot j}} \right) + \frac{1}{N \cdot p_{iN}} - \frac{1}{N^2 \cdot \bar{p}_{\cdot N}} \\ &= \delta_{j,t} \frac{\sum_{k=1}^{N-1} p_{kj} - p_{ij}}{N^2 \cdot p_{ij} \cdot \bar{p}_{\cdot j}} + \frac{\sum_{k=1}^{N-1} p_{kN} - p_{iN}}{N^2 \cdot p_{iN} \cdot \bar{p}_{\cdot N}} \\ &= \delta_{j,t} \frac{\sum_{k \neq i} p_{kj}}{N^2 \cdot p_{ij} \cdot \bar{p}_{\cdot j}} + \frac{\sum_{k \neq i} p_{kN}}{N^2 \cdot p_{iN} \cdot \bar{p}_{\cdot N}} \geq 0, \end{aligned} \quad (\text{A6})$$

but when $i \neq s$,

$$\frac{\partial^2 EI}{\partial p_{ij} \partial p_{st}} = -\frac{\delta_{j,t}}{N^2 \cdot \bar{p}_{\cdot j}} - \frac{1}{N^2 \cdot \bar{p}_{\cdot N}} \leq 0 \quad (\text{A7})$$

holds, no matter if $j = t$ or not. Therefore, the Hessian matrix of EI is not positive-definite, EI is not a convex function. \square

We will further discuss the condition and the properties of the maximum of EI .

Proposition 2. *The EI measure can reach its maximum $\log N$ if and only if P is a permutation matrix.*

Proof. By noticing that

$$\begin{aligned} \sum_{i=1}^N \sum_{j=1}^N p_{ij} \log \bar{p}_{\cdot j} &= \sum_{j=1}^N \left(\sum_{i=1}^N p_{ij} \right) \log \bar{p}_{\cdot j} \\ &= \sum_{j=1}^N \bar{p}_{\cdot j} \log \bar{p}_{\cdot j} = -H(\bar{P}), \end{aligned} \quad (\text{A8})$$

where $H(\bar{P})$ is the Shannon entropy of the average distribution $\bar{P} \equiv \sum_{i=1}^N P_i/N$. Thus, the EI can also be separated as:

$$\begin{aligned} EI &= \frac{1}{N} \sum_{i=1}^N \sum_{j=1}^N p_{ij} \log p_{ij} - \frac{1}{N} \sum_{i=1}^N \sum_{j=1}^N \bar{p}_{\cdot j} \log \bar{p}_{\cdot j} \\ &= \frac{1}{N} \sum_{i=1}^N (-H(P_i)) + H(\bar{P}). \end{aligned} \quad (\text{A9})$$

Where $H(P_i) = -\sum_{j=1}^N p_{ij} \log p_{ij}$ is the Shannon entropy of the distribution P_i . Furthermore, we have:

$$-H(P_i) \leq 0, \quad (\text{A10})$$

the equality holds when P_i is a one hot vector, and we also have:

$$H(\bar{P}) \leq \log N, \quad (\text{A11})$$

and the equality holds when $\bar{P} = \frac{1}{N} \cdot \mathbb{1}$. By combining these two inequality together, we can obtain:

$$EI \leq 0 + \log N = \log N. \quad (\text{A12})$$

The condition that make the equality in Equation A10 and the equality in Equation A11 hold simantaneously is that all row vectors in P are one-hot vectors, and they are all different such that

$$\frac{1}{N} \sum_i P_i = \bar{P} = \frac{1}{N} \cdot \mathbb{1}. \quad (\text{A13})$$

Therefore, we reach the statement claimed by this theorem that P must be a permutation matrix. □

A.2 Theorems and proves for dynamical reversibility and Γ

A.2.1 Dynamical Reversibility and Time Reversibility

Theorem 1. *For a given markov chain χ and the corresponding TPM P , if P is dynamically reversible as defined in Definition 1, if and only if P is a permutation matrix.*

Proof. If P is dynamical reversible, then P must be an invertible matrix and P is a TPM (which means all row vectors are normalized $|P_i|_1 = 1$).

Because P is invertible, therefore,

$$P = U \cdot \text{diag}(\lambda_1, \lambda_2, \dots, \lambda_N) \cdot U^{-1}, \quad (\text{A14})$$

where, U is an orthonormal matrix, $\lambda_1, \lambda_2, \dots, \lambda_N$ are the eigenvalues of P , and their modulus are less than or equal to 1:

$$|\lambda_i| \leq 1, \forall i \in [1, N], \quad (\text{A15})$$

these inequality holds because P is a TPM of a Markov chain according to [31].

Thus, the inverse of P can be expressed by:

$$P^{-1} = U \cdot \text{diag}(\lambda_1^{-1}, \lambda_2^{-1}, \dots, \lambda_N^{-1}) \cdot U^{-1}, \quad (\text{A16})$$

and:

$$|\lambda_i|^{-1} \geq 1, \forall i \in [1, N], \quad (\text{A17})$$

However, this conflicts with the conclusion that the modulus of all the eigenvalues of a TPM must be less or equals to 1 if the inequality holds strictly. Thus, we have:

$$|\lambda_1| = |\lambda_2| = \cdots = |\lambda_N| = 1. \quad (\text{A18})$$

Therefore, the eigenvalues are the complex solutions for the equation of $x^N = 1$, thus P is a permutation matrix.

On the other hand, if P is a permutation matrix, then it is invertible because permutation matrices are full rank and eigenvalues are 1. The normalization conditions $|P_i|_1, \forall i \in [1, N]$ are satisfied because all row vectors P_i are one-hot vectors. Therefore, P is dynamical reversible. \square

Next, we will prove dynamical reversibility implies time reversibility for Markov chains.

Proposition 3. *For a recurrent discrete Markov chain χ , suppose its TPM is P on the space of states \mathcal{S} and its stationary distribution is μ , if P is dynamically reversible, then χ also satisfies time reversibility.*

Proof. Suppose χ 's time reversed Markov chain is χ' , and its TPM $Q_{ij} \equiv P(X_t = s_i | X_{t+1} = s_j)$, where s_i and $s_j \in \mathcal{S}$ are the states at time steps t and $t+1$, respectively. Then P, Q, μ should satisfy the detailed balance condition:

$$P(X_{t+1}, X_t) = P(X_t, X_{t+1}), \quad (\text{A19})$$

By using Bayesian formulation,

$$P(X_t, X_{t+1}) = P(X_{t+1}|X_t)P(X_t) = P(X_{t+1})P(X_t|X_{t+1}), \quad (\text{A20})$$

and let $t \rightarrow \infty$ such that $P(X_t) = P(X_{t+1}) = \mu$, Equation A20 can be written as:

$$Q_{ij} \cdot \mu_i = P_{ji} \cdot \mu_j \quad (\text{A21})$$

If χ is time reversible, then $Q = P$, therefore:

$$P_{ij} \cdot \mu_i = P_{ji} \cdot \mu_j. \quad (\text{A22})$$

Equation A22 is the sufficient and necessary condition for χ being time reversible.

If P is dynamically reversible, then P is a permutation matrix according to Theorem 1, thus, the corresponding stationary distribution must be $\mathbb{1}/N$ such that any permutation on elements in $\mathbb{1}/N$ is the same vector.

Because P is invertible, it satisfies

$$P = P^{-1} = P^T, \quad (\text{A23})$$

then by taking Equation A23 and the stationary distribution into Equation A22, we have

$$left = P_{ij} \cdot \frac{\mathbb{1}}{N} = P_{ji} \cdot \frac{\mathbb{1}}{N} = right. \quad (\text{A24})$$

Therefore, the dynamical reversibility of χ implies its time reversibility. But its reverse is not, apparently. \square

A.2.2 Approximate Dynamical Reversibility Γ_α

We will present the propositions and theorems and the proves about the measure of approximate dynamical reversibility Γ_α in this sub-section. Before the propositions are presented, we will prove the lemma related with the proposition that will be used in the following parts.

Lemma 1. For a TPM $P = (P_1, P_2, \dots, P_N)^T$, where P_i is the i -th row vector, then:

$$P_i \cdot P_j \leq 1, \forall i, j \in [1, N] \quad (\text{A25})$$

Proof. Because P_i is a probability distribution, therefore, it should satisfy normalization condition which can be expressed as:

$$|P_i|_1 = \sum_{j=1}^N p_{ij} = 1, \quad (\text{A26})$$

where, $|\cdot|_1$ is 1-norm for vector, which is defined as the summation of the absolute values of all elements. Thus:

$$P_i \cdot P_j = |P_i \cdot P_j|_1 \leq |P_i|_1 \cdot |P_j|_1 = 1. \quad (\text{A27})$$

\square

Proposition 4. For a given TPM P , suppose its singular values are $(\sigma_1, \sigma_2, \dots, \sigma_N)$, we have:

$$\sum_{i=1}^N \sigma_i^2 = \sum_{i=1}^N P_i^2 = \|P\|_F^2 \leq N, \quad (\text{A28})$$

and the equality holds when $P_i, \forall i \in [1, N]$ are one-hot vectors.

Proof. Because $\sigma_i^2, \forall i \in [1, N]$ are the eigenvalues of $P \cdot P^T$, thus, P can be written:

$$P \cdot P^T = U \Sigma^2 U^T, \quad (\text{A29})$$

where U is a orthonormal matrix with size N , $\Sigma^2 = \text{diag}(\sigma_1^2, \sigma_2^2, \dots, \sigma_N^2)$. Thus,

$$\begin{aligned} \sum_{i=1}^N \sigma_i^2 &= \text{Tr} \Sigma^2 = \text{Tr} (U \Sigma^2 U^T) = \text{Tr} (P \cdot P^T) \\ &= \sum_{i=1}^N P_i^2 \leq N. \end{aligned} \quad (\text{A30})$$

The last inequality holds because of Lemma 1. And the equality holds if and only if:

$$P_i \cdot P_i = 1, \forall i \in [1, N], \quad (\text{A31})$$

that is $P_i, \forall i \in [1, N]$ are one-hot vectors.

Further, it should be noticed that:

$$\sum_{i=1}^N \sigma_i^2 = \sum_{i=1}^N P_i^2 = \sum_{i=1}^N \sum_{j=1}^N p_{ij}^2 = \|P\|_F^2 \quad (\text{A32})$$

Therefore, Equation A28 holds, and the equality in Equation A30 holds when all row vectors are one-hot vectors. \square

Lemma 2. For a TPM P , we can write it in the following way:

$$P = (P_1, P_2, \dots, P_N)^T, \quad (\text{A33})$$

where P_i is the i -th row vector. And suppose P 's singular values are $\sigma_1 \geq \sigma_2 \geq \dots \geq \sigma_N$. Thus, if

$$P_i \cdot P_i = 1, \forall i \in [1, N], \quad (\text{A34})$$

then the singular values of P satisfy:

$$\sigma_1 \geq \sigma_2 \geq \dots \geq \sigma_r \geq 1 \quad (\text{A35})$$

and

$$\sigma_{r+1} = \sigma_{r+2} = \dots = \sigma_N = 0, \quad (\text{A36})$$

where r is the rank of the matrix P .

Proof. If $P_i \cdot P_i = 1$, then $\sum_j p_{ij}^2 = 1$, that means P_i is a unit vector with modulus 1. While, $|P_i|_1 = \sum_{j=1}^N p_{ij} = 1$ for all i , so P_i must be a one hot vector which means only one element is 1 and others are zeros.

Therefore, there are two cases for P : 1. There are $1 \leq i, j \leq N$, such that $P_i = P_j$; 2. For any $1 \leq i, j \leq N$, $P_i \neq P_j$.

Case 1: If $P_i = P_j$ and because both of them are one-hot vectors, therefore $P_i \cdot P_j = 1$ and $P_j \cdot P_i = 1$ due to the symmetry of inner product. Therefore, both the element at the i th row and j th column and the element at the j th row and i th column are ones, and others are zeros. Notice that, $P_i \cdot P_i = 1$ holds in the same time according to the condition, thus, the matrix of $P \cdot P^T$ has the following form:

$$P \cdot P^T = \begin{matrix} & & & & i & & j & & \\ & & & & & & & & \\ & & & & & & & & \\ & & & & & & & & \\ & & & & & & & & \\ i & & & & & & & & \\ & & & & & & & & \\ & & & & & & & & \\ j & & & & & & & & \\ & & & & & & & & \end{matrix} \begin{pmatrix} 1 & \dots \\ \dots & \ddots & \dots & \dots & \dots & \dots & \dots & \dots \\ \dots & \dots & 1 & \dots & 1 & \dots & \dots & \dots \\ \dots & \dots & \dots & \ddots & \dots & \dots & \dots & \dots \\ \dots & \dots & 1 & \dots & 1 & \dots & \dots & \dots \\ \dots & \dots \end{pmatrix}, \quad (\text{A37})$$

in which, all the elements are 0 except the diagonal entries and the elements at i, j and j, i .

From Equation A37, we know that the i th row is identical to the j th row. Thus, the minimum eigenvalue of PP^T which is also the last singular value of P must be 0.

If there are multiple (say $N - r$) pairs of (i, j) and $i \neq j$ which satisfies $P_i \cdot P_j = 1$, then the last $N - r$ singular values are all zeros. And the rank of P is r . Therefore:

$$\sigma_{r+1} = \sigma_{r+2} = \cdots = \sigma_N = 0. \quad (\text{A38})$$

In this case, $P \cdot P^T$ can be written as:

$$P \cdot P^T = \begin{pmatrix} I_{(r-1) \times (r-1)}, & \mathbb{O}_{(r-1) \times (N-r+1)} \\ \mathbb{O}_{(N-r+1) \times (r-1)}, & \mathbb{1}_{(N-r+1) \times (N-r+1)} \end{pmatrix}, \quad (\text{A39})$$

where $I_{(r-1) \times (r-1)}$ is an identity matrix with size $(r-1) \times (r-1)$, and \mathbb{O} and $\mathbb{1}$ are the matrices with all elements being 0 and 1. As a result, the singular values of P with a decreasing order is:

$$\sigma = \left(\sqrt{N-r+1}, \underbrace{1, 1, \dots, 1}_{r-1}, \underbrace{0, 0, \dots, 0}_{N-r} \right). \quad (\text{A40})$$

Therefore:

$$\sigma_1 \geq \sigma_2 \geq \cdots \geq \sigma_r \geq 1, \quad (\text{A41})$$

Case 2: If $P_i \cdot P_j = 1$ holds only for $i = j$, then the non-zero elements all locate on the diagonal of PP^T , thus, $PP^T = I$. In this case $P^T = P^{-1}$, and P must be a permutation matrix, and all singular values are 1. This is also in accordance with the statement of Lemma 2. □

We want to prove that it is reasonable that the proposed measure Γ_α to characterize the dynamical reversibility. First, we will prove that Γ_α is upper bounded by the system size N , and it can reach the maximum value if and only if P is reversible.

Lemma 3. For a given TPM P , the measure of dynamical reversibility Γ_α for any $\alpha \in (0, 2)$, is less than or equal to the size of the system N .

Proof. Because $0 < \alpha < 2$, $f(x) = x^{\alpha/2}$ is a concave function, and according to Proposition 4, we have:

$$\begin{aligned} \Gamma_\alpha &= \sum_{i=1}^N \sigma_i^\alpha = N \cdot \frac{\sum_{i=1}^N \sigma_i^{2 \cdot \frac{\alpha}{2}}}{N} \leq N \left(\frac{\sum_{i=1}^N \sigma_i^2}{N} \right)^{\alpha/2} \\ &= N^{1-\alpha/2} \left(\sum_{i=1}^N P_i^2 \right)^{\alpha/2} \leq N^{1-\frac{\alpha}{2} + \frac{\alpha}{2}} = N \end{aligned} \quad (\text{A42})$$

□

Next, we will discuss about the upper bound of Γ_α .

Theorem 2. *The maximum of Γ_α is N for any $\alpha \in (0, 2)$, and it can be achieved if and only if P is a permutation matrix.*

Proof. First, we will prove that when the maximum N is achieved for Γ_α , P must be a permutation matrix.

Notice that the condition for P_i to satisfy the equality in the second inequality of Equation A42 is $P_i^2 = 1$ for all $i \in [1, N]$.

Therefore, according to Lemma 2, there are two cases need to be discussed separately.

Case 1: If there are two rows of P are identical: $P_i \cdot P_j = 1$ for some i, j , then the rank of P is $r < N$. Then, according to Lemma 2 the first r singular values satisfy:

$$\sum_{i=1}^r \sigma_i^2 = N, \quad (\text{A43})$$

and $\sigma_i \geq 1$ for any $i \in [1, r]$.

Suppose there are $s \leq r$ singular values strictly larger than 1, then $\sigma_i^2 > \sigma_i^\alpha$ for those $1 \leq i \leq s$, thus:

$$\sum_{i=1}^s \sigma_i^\alpha < \sum_{i=1}^s \sigma_i^2, \quad (\text{A44})$$

And for $i > s$, the singular values are either 0 or 1, and therefore $\sigma_i = \sigma_i^2$. Finally, we have:

$$\Gamma_\alpha = \sum_{i=1}^N \sigma_i^\alpha < \sum_{i=1}^N \sigma_i^2 = N, \quad (\text{A45})$$

Thus, in this case, the equality in Equation A42 does not hold.

Case 2: If $P_i \cdot P_j \neq 1$ for any $i \neq j$, and $P_i \cdot P_i = 1$ for $\forall i \in [1, N]$, then according to Lemma 2, if and only if all the singular values are 1, that is,

$$\sigma_i = \sigma_j = 1, \forall i, j \in [1, N], \quad (\text{A46})$$

which implies P is invertible. Notice that, this is exactly the same condition to make the equality holds for the first inequality in Equation A42.

Second, we will prove the necessity for the maximum of Γ_α . If P is a permutation matrix, the eigenvalues of P are the singular values because P is symmetric. And the singular values satisfy:

$$\sigma_1 = \sigma_2 = \dots = \sigma_N = 1, \quad (\text{A47})$$

thus,

$$\Gamma_\alpha = \sum_{i=1}^N \sigma_i^\alpha = N \quad (\text{A48})$$

which achieves the maximum value of Γ_α . □

This theorem implies $\sum_i \sigma_i^\alpha$ is a better indicator for approximate dynamical reversibility than $\sum_i \sigma_i^2$ for $\alpha < 2$ although both of them can achieve the maximized value N when P is reversible. However, if P is degenerative, $\sum_i \sigma_i^2$ is also N , but $\sum_i \sigma_i^\alpha$ is not.

Next, we will discuss the minimum value and minimum point of Γ_α .

Lemma 4. *The rank of a nonzero TPM P can achieve the minimum value of 1 if and only if the row vectors of P_i for any i are identical. In this case,*

$$\Gamma_\alpha = |P_1|^\alpha \cdot N^{\alpha/2} \quad (\text{A49})$$

Proof. If the rank of P is 1, all the $N-1$ row vectors of $P_i, \forall i \in [1, N]$ can be expressed by a linear function of the first row vector P_1 , thus

$$P_i = k \cdot P_1, \quad (\text{A50})$$

with $k > 0$. However, because $|P_i|_1 = 1$, thus k must be one. Therefore:

$$P_i = P_j, \forall i, j \in [1, N]. \quad (\text{A51})$$

On the other hand, if Equation A51 holds, the rank of P should be 1.

In this case,

$$P \cdot P^T = |P_1|^2 \cdot \mathbb{1}_{N \times N}, \quad (\text{A52})$$

where $|\cdot|$ is the modulus for \cdot . Therefore, the eigenvalues of $P \cdot P^T$ are $(|P_1|^2 \cdot N, 0, \dots, 0)$. Thus, the singular values of P should be $(|P_1| \cdot \sqrt{N}, 0, \dots, 0)$, this leads to Equation A49 \square

Proposition 5. *For a given TPM $P = (P_1, P_2, \dots, P_N)^T$, $\Gamma_\alpha = \sum_{i=1}^N \sigma_i^\alpha$ can reach its minimum 1 if and only if $P_i = \frac{1}{N}(1, 1, \dots, 1)$ for $\forall i \in [1, N]$.*

Proof. When $P_i = \frac{1}{N}(1, 1, \dots, 1)$ for $\forall i \in [1, N]$, $|P_1| = N^{-1/2}$, and according to Lemma 4,

$$\Gamma_\alpha = \sum_{i=1}^N \sigma_i^\alpha = |P_1|^\alpha \cdot N^{\alpha/2} = N^{-\alpha/2} \cdot N^{\alpha/2} = 1 \quad (\text{A53})$$

for any $0 \leq \alpha < 2$.

On the other hand, because the minimum value of σ_i is zero, and $\Gamma_\alpha = \sum_i \sigma_i^\alpha \geq 0$, thus Γ_α can be minimized if the number of zero singular values is maximized. Notice that the number of non-zero singular values of P is the same as the rank of P . Thus, the minimum of Γ_α can be reached when the minimized rank of P is reached. In such case, according to Lemma 4, $\Gamma_\alpha = |P_1|^\alpha \cdot N^{\alpha/2}$, thus the minimized value of Γ_α is solely dependent on $|P_1|$. While, because P_1 is a probability distribution which satisfies $|P_i|_1 = 1$, thus, $P_1 \cdot P_1$ can be minimized when all the elements are equal. Thus,

$$P_1 = \frac{1}{N} \cdot \mathbb{1}. \quad (\text{A54})$$

Therefore, $\frac{1}{N} \cdot \mathbb{1}$ is the minimum point. \square

Next, to illustrate why the dynamics reversibility measure Γ_α increases as the probability matrix P asymptotically converges to a permutation matrix, or dynamically reversible, we have the following lemmas and the theorem.

Lemma 5. *The function of $f(\alpha) = \left(\sum_{i=1}^N x_i^\alpha\right)^{1/\alpha}$ is a monotonic decreasing function of α for any $x_i \geq 0, \forall i \in [1, N]$ and $\alpha > 0$.*

Proof. Because:

$$\sum_{i=1}^N (x_i^\alpha)^2 \leq \left(\sum_{i=1}^N x_i^\alpha\right)^2, \quad (\text{A55})$$

thus:

$$\log \frac{\sum_{i=1}^N x_i^{2\alpha}}{\sum_{i=1}^N x_i^\alpha} \leq \log \sum_{i=1}^N x_i^\alpha. \quad (\text{A56})$$

Further, because \log is a concave function, therefore:

$$\sum_{i=1}^N \left(\frac{x_i^\alpha}{\sum_{j=1}^N x_j^\alpha}\right) \cdot \log x_i^\alpha \leq \log \sum_{i=1}^N \left(\frac{x_i^\alpha}{\sum_{j=1}^N x_j^\alpha} \cdot x_i^\alpha\right), \quad (\text{A57})$$

thus, combining Eq. A56 and A57, we have:

$$\frac{\sum_{i=1}^N x_i^\alpha \cdot \log x_i^\alpha}{\sum_{i=1}^N x_i^\alpha} \leq \log \sum_{i=1}^N x_i^\alpha. \quad (\text{A58})$$

The equality holds when $x_i = 0, \forall i \in [1, N]$. Notice that the right hand term is $-\left(\frac{1}{\alpha}\right)' \log \sum_{i=1}^N x_i^\alpha$, and the left hand term is $\frac{1}{\alpha} \cdot \left(\log \sum_{i=1}^N x_i^\alpha\right)'$, thus Equation A58 implies:

$$\left(\frac{1}{\alpha} \cdot \log \sum_{i=1}^N x_i^\alpha\right)' = \frac{1}{\alpha} \cdot \left(\log \sum_{i=1}^N x_i^\alpha\right)' + \left(\frac{1}{\alpha}\right)' \log \sum_{i=1}^N x_i^\alpha \leq 0. \quad (\text{A59})$$

Therefore, $\log f(\alpha) = \frac{1}{\alpha} \cdot \left(\log \sum_{i=1}^N x_i^\alpha\right)$ is a monotonic decreasing function of α , and so does $f(\alpha) = \left(\sum_{i=1}^N x_i^\alpha\right)^{1/\alpha}$. \square

Proposition 6. *The approximate dynamical reversibility measure Γ_α is lower bounded by $\|P\|_F^\alpha$.*

Proof. Because $0 < \alpha < 2$ and $\sigma_i \geq 0, \forall i \in [1, N]$ but the equality can not be hold for all $i \in [1, N]$, this means $f(\alpha) = \left(\sum_{i=1}^N \sigma_i^\alpha\right)^{1/\alpha}$ is a strict monotonic decreasing function of α according to Lemma 5, thus:

$$\Gamma_\alpha^{1/\alpha} = \left(\sum_{i=1}^N \sigma_i^\alpha\right)^{1/\alpha} \geq \left(\sum_{i=1}^N \sigma_i^2\right)^{1/2}, \quad (\text{A60})$$

the equality holds only when $\sigma_i = 1$ or 0 for all $i \in [1, N]$. According to Proposition 4:

$$\left(\sum_{i=1}^N \sigma_i^2 \right)^{1/2} = \left(\sum_{i=1}^N P_i^2 \right)^{1/2} = [\text{Tr}(P \cdot P^T)]^{1/2}. \quad (\text{A61})$$

While,

$$\sqrt{\sum_{i=1}^N P_i^2} = \sqrt{\sum_i^N \sum_j^N P_{ij}^2} = \|P\|_F \quad (\text{A62})$$

Therefore:

$$\Gamma_\alpha \geq [\text{Tr}(P \cdot P^T)]^{\alpha/2} = \|P\|_F^\alpha. \quad (\text{A63})$$

□

As P_i can achieve its maximum when it is a one-hot vector, therefore the lower bound of Γ_α increases as P approaches a matrix with one-hot row vectors. This can be concluded as a following proposition:

Proposition 7. *The lower bound of the approximate dynamical reversibility measure Γ_α is increased with the number of one hot vectors in the TPM P .*

Proof. Because $|P_i|_1 = 1$ for all $1 \leq i \leq N$, therefore $\|P_i\|^2 \leq 1$ and the equality holds if and only if P_i is a one-hot vector. Further, according to Proposition 6, we have:

$$\Gamma_\alpha \geq [\text{Tr}(P \cdot P^T)]^{\alpha/2} = \left(\sum_{i=1}^N P_i^2 \right)^{\alpha/2}. \quad (\text{A64})$$

Thus, the lower bound $\left(\sum_{i=1}^N P_i^2 \right)^{\alpha/2}$ increased as each row vector $P_i, \forall i \in [1, N]$ converges to a one-hot vector. □

However, P may not be a permutation matrix because some row vectors may be similar, which means P_i for all $i \in [1, N]$ are not orthogonal each other but they collapse to one direction. Thus, we need to further prove a proposition to exclude this case.

Proposition 8. *If P is formed by one-hot vectors, and the rank is r , then Γ_α is $(N - r - 1)^\alpha + r$, and this value increases with r .*

Proof. If P is formed by one-hot vectors, and $r - 1 \in [1, N]$ of them are orthogonal each other, the left $N - r + 1$ of them are identical. Without losing generality, the TPM P can be written as:

$$P = \begin{pmatrix} I_{(r-1) \times (r-1)}, & \mathbb{O}_{(r-1) \times (N-r+1)} \\ \mathbb{O}_{(N-r+1) \times (r-1)}, & e^{(N)_{(N-r+1)}} \end{pmatrix}, \quad (\text{A65})$$

where, $\mathbb{O}_{m \times n}$ represents a matrix with size $m \times n$ and all elements being 0, and $e^{(N)_{(N-r+1)}}$ represents $(N - r + 1)$ one-hot vectors with the N th elements are all ones

and other elements are zeros. Thus, $P \cdot P^T$ is:

$$P \cdot P^T = \begin{pmatrix} I_{(r-1) \times (r-1)}, & \mathbb{O}_{(r-1) \times (N-r+1)} \\ \mathbb{O}_{(N-r+1) \times (r-1)}, & \mathbb{1}_{(N-r+1) \times (N-r+1)} \end{pmatrix}, \quad (\text{A66})$$

as a result, the singular values of P with a decreasing order is:

$$\sigma = \left(\sqrt{N-r+1}, \underbrace{1, 1, \dots, 1}_{r-1}, \underbrace{0, 0, \dots, 0}_{N-r} \right). \quad (\text{A67})$$

Therefore, Γ_α can be derived in this special case:

$$\Gamma_\alpha(r) = (N-r+1)^{\alpha/2} + r - 1, \quad (\text{A68})$$

By taking the derivative of Equation A68 with respect to r to get a positive result, thus $\Gamma_\alpha(r)$ is a monotonic increasing function with respect to r . \square

In conclusion, to maximize Γ_α for any given P , we should initially augment the number of one-hot vectors in P , as highlighted in Proposition 7. Subsequently, we can proceed by transforming an increasing number of one-hot vectors into mutually orthogonal base vectors according to Proposition 8.

A.3 Comparison between $\log \Gamma_\alpha$ and EI

In this subsection, we will establish the relationship between $\log \Gamma_\alpha$ and EI . First, we can synthesize the theoretical results about the minimum and maximum for both Γ_α and EI to derive the following theorem:

Theorem 3: For any TPM P and $\alpha \in (0, 1)$, both the logarithm of Γ_α and EI share identical minimum value of 0 and one common minimum point at $P = \frac{1}{N} \mathbb{1}_{N \times N}$. They also exhibit the same maximum value of $\log N$ with maximum points corresponding to P being a permutation matrix.

Proof. According to Proposition 1, EI has the minimum 0 when P has identical row vectors, and $P = \frac{1}{N} \cdot \mathbb{1}_{N \times N}$ satisfies this condition. While, according to Proposition 5, $\log \Gamma_\alpha$ has also the minimum value 0 when $P = \frac{1}{N} \cdot \mathbb{1}_{N \times N}$. Therefore, EI and $\log \Gamma_\alpha$ share the same minimum.

On the other hand, according to Proposition 2, EI has the same maximum at $\log N$ when P is a permutation matrix. So does $\log \Gamma_\alpha, \forall \alpha \in (0, 2)$ according to Theorem 2.

Therefore, EI and $\log \Gamma_\alpha$ share the same minimum and maximum for any $\alpha \in (0, 2)$. \square

We will prove a theorem that EI is upper bounded by $\frac{2}{\alpha} \log \Gamma_\alpha$.

Theorem 4. For any TPM P , its effective information EI is upper bounded by $\frac{2}{\alpha} \log \Gamma_\alpha$, and lower bounded by $\log \Gamma_\alpha - \log N$.

Proof. First, because the upper bound of the average distribution \bar{P} is:

$$H(\bar{P}) \leq \log N, \quad (\text{A69})$$

the equality holds when \bar{P} is $\frac{1}{N} \cdot \mathbf{1}$. Second, according to the concavity of \log function, we have:

$$\begin{aligned} -\frac{1}{N} \sum_{i=1}^N H(P_i) &= \frac{1}{N} \sum_{i=1}^N \sum_{j=1}^N p_{ij} \log p_{ij} \\ &\leq \frac{1}{N} \sum_{i=1}^N \log \left(\sum_{j=1}^N p_{ij}^2 \right) \\ &\leq \log \sum_{i=1}^N \sum_{j=1}^N p_{ij}^2 - \log N, \end{aligned} \quad (\text{A70})$$

and the equality holds when $p_{ij} = 1/N$ for all $1 \leq i, j \leq N$. Thus, we bring the two inequalities (Equation A69 and Equation A70) into Equation A9, we obtain:

$$EI = -\frac{1}{N} \sum_{i=1}^N H(P_i) + H(\bar{P}) \leq \log \sum_{i=1}^N \sum_{j=1}^N p_{ij}^2. \quad (\text{A71})$$

This is the upper bound of EI and the equality holds when $P = \frac{1}{N} \cdot \mathbf{1}_{N \times N}$.

On the other hand, according to Proposition 5,

$$\log \Gamma_\alpha = \log \sum_{i=1}^N \sigma_i^\alpha \geq \log \|P\|_F^\alpha = \frac{\alpha}{2} \log \sum_{i=1}^N \sum_{j=1}^N p_{ij}^2, \quad (\text{A72})$$

the equality holds when $\sigma_i = 0, 1, \forall i \in [1, N]$. Therefore:

$$EI \leq \frac{2}{\alpha} \log \Gamma_\alpha. \quad (\text{A73})$$

Furthermore, because $EI \geq 0$ and $\Gamma_\alpha \leq N$, thus:

$$EI - \log \Gamma_\alpha \geq 0 - \log N = -\log N \quad (\text{A74})$$

Therefore,

$$EI \geq \log \Gamma_\alpha - \log N, \quad (\text{A75})$$

Thus, EI is lower bounded by $\log \Gamma_\alpha - \log N$. \square

Tighter bounds are expected to be found in future works.

A.3.1 Quantification for causal emergence

Proposition 9. For any given TPM P with singular values $\sigma_1 \geq \sigma_2 \geq \dots \geq \sigma_N$ and rank r , and for any given $\epsilon \in [0, \sigma_1]$, the degree of causal emergence of P is:

$$\Delta\Gamma_\alpha = \frac{\sum_{i=1}^{r_\epsilon} \sigma_i^\alpha}{r_\epsilon} - \frac{\sum_{i=1}^N \sigma_i^\alpha}{N}, \quad (\text{A76})$$

and this degree satisfies the following inequality:

$$0 \leq \Delta\Gamma_\alpha \leq N - 1, \quad (\text{A77})$$

where $r_\epsilon = \max\{i | \sigma_i > \epsilon\}$.

Proof. When $\epsilon \in (\sigma_N, \sigma_1]$, there is an integer $i \in (1, N]$ such that $\sigma_i > \epsilon$, and r_ϵ is the maximum one to satisfy this condition. Therefore:

$$\sigma_1 \geq \sigma_2 \geq \dots \geq \sigma_{r_\epsilon} > \epsilon \geq \sigma_{r_\epsilon+1} \geq \dots \geq \sigma_N \geq 0, \quad (\text{A78})$$

thus:

$$\sum_{i=1}^{r_\epsilon} \sigma_i^\alpha > r_\epsilon \cdot \epsilon^\alpha, \quad (\text{A79})$$

and:

$$- \sum_{i=r_\epsilon+1}^N \sigma_i^\alpha \geq -(N - r_\epsilon) \cdot \epsilon^\alpha. \quad (\text{A80})$$

Therefore:

$$\frac{\sum_{i=1}^{r_\epsilon} \sigma_i^\alpha}{r_\epsilon} - \frac{\sum_{i=1}^N \sigma_i^\alpha}{N} = \sum_{i=1}^{r_\epsilon} \sigma_i^\alpha \left(\frac{1}{r_\epsilon} - \frac{1}{N} \right) - \frac{\sum_{i=r_\epsilon+1}^N \sigma_i^\alpha}{N} > r_\epsilon \epsilon^\alpha \left(\frac{1}{r_\epsilon} - \frac{1}{N} \right) - \frac{(N - r_\epsilon) \cdot \epsilon^\alpha}{N} = 0. \quad (\text{A81})$$

While, when $\epsilon < \sigma_N$, $r_\epsilon = N$, so $\Delta\Gamma_\alpha = 0$, therefore:

$$\Delta\Gamma_\alpha \geq 0 \quad (\text{A82})$$

On the other hand, because $r_\epsilon \leq N$, and according to Theorem 2, thus:

$$\sum_{i=1}^{r_\epsilon} \sigma_i^\alpha \leq \sum_{i=1}^N \sigma_i^\alpha \leq N. \quad (\text{A83})$$

Since $1 \leq r_\epsilon \leq N$, therefore

$$0 \leq \frac{1}{r_\epsilon} - \frac{1}{N} \leq 1 - \frac{1}{N}. \quad (\text{A84})$$

Thus,

$$\frac{\sum_{i=1}^{r_\epsilon} \sigma_i^\alpha}{r_\epsilon} - \frac{\sum_{i=1}^N \sigma_i^\alpha}{N} \leq \sum_{i=1}^N \sigma_i^\alpha \left(\frac{1}{r_\epsilon} - \frac{1}{N} \right) \leq N - 1. \quad (\text{A85})$$

Combining Equation A81 and A85, we obtain Equation A77 \square

Proposition 10. *For any given TPM P with singular values $\sigma_1 \geq \sigma_2 \geq \dots \geq \sigma_N$ and rank r , according to Definition 4, causal emergence occurs if and only if $\Delta\Gamma_\alpha(\epsilon) > 0$ for any $\epsilon \geq 0$.*

Proof. Case I: When $\epsilon > 0$, according to Definition 4, if there exists an integer $i \in [1, N)$ such that $\sigma_i > \epsilon$ for any $\epsilon \in [0, \sigma_1]$, that is $\epsilon > \sigma_N$, then the vague CE occurs. Then, according to Proposition 9, $\Delta\Gamma_\alpha(\epsilon) > 0$ in this case.

Otherwise, if $\Delta\Gamma_\alpha(\epsilon) > 0$, then $r_\epsilon < N$, where $r_\epsilon = \max\{i | \sigma_i > \epsilon\}$, and therefore $\sigma_{r_\epsilon} > \epsilon$. According to Definition 4, vague CE occurs.

Case II: When $\epsilon = 0$, according to Definition 3, the rank r of P is less than N and $\sigma_j = 0, \forall j \in [r + 1, N]$, therefore

$$\frac{\sum_{i=1}^r \sigma_i^\alpha}{r} > \frac{\sum_{i=1}^N \sigma_i^\alpha}{N}, \quad (\text{A86})$$

so $\Delta\Gamma_\alpha > 0$.

Otherwise, if $\Delta\Gamma_\alpha > 0$, there exists $r_{\epsilon=0} < N$ such that $r_{\epsilon=0} = \max\{i | \sigma_i > 0\}$. Thus, $\sigma_i = 0, \forall i > r_{\epsilon=0}$, that is $r_{\epsilon=0}$ is the rank of the matrix P . Therefore, clear CE occurs according to Definition 3. \square

Appendix B Experiments on testing the correlation between EI and Γ

In this section of the appendix, we will introduce the details of our experiments on the relationship between the approximate dynamical reversibility Γ and EI on various generated TPMs. The generative model of TPMs have three classes: softening of permutation matrix, softening of controlled degenerative TPMs, and random normalized.

B.1 Softening of Permutation Matrix

In this series experiments, we will find out what the relationships between Γ and EI are on a variety of TPMs with different deviations from the reversible TPMs (permutation matrix) and different sizes.

For given size N , The TPM is generated by three steps: 1). Randomly sample a permutation matrix with dimension $N \times N$; 2). For each row vector P_i in P , suppose the position of the 1 element is j_i , we fill out all entries of P_i with the probabilities of a Gaussian distribution center at j_i , that is, $P'_{i,j} = \frac{1}{\sqrt{2\pi}\sigma} \exp -\frac{(j-j_i)^2}{\sigma^2}$, where, σ is a free parameter for the degree of softening; 3). Normalize this new row vector P'_i by dividing $\sum_{j=1}^N P'_{ij} = 1$, such that the modified matrix P' is also a TPM.

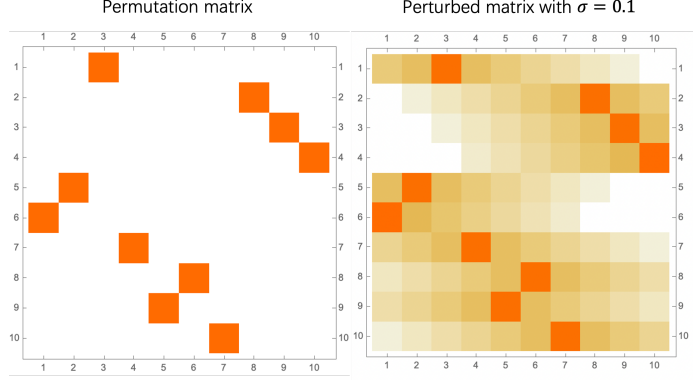


Fig. S1 The original TPM and the perturbed one.

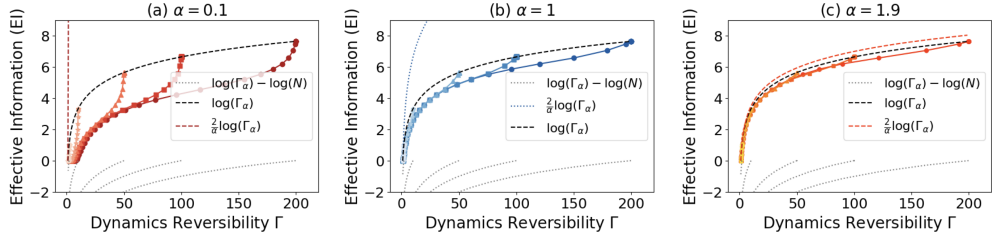


Fig. S2 The relationships between EI and Γ_α for different α . The theoretical and empirical upper bounds are shown as red and black dashed lines, while the theoretical lower bounds which change with N are also shown as dotted lines.

In this model, the unique parameter σ can control the degree of deviations from the original TPM. When $\sigma = 0$, we recover the original TPM. And when σ increases to very large value, then the row vectors converge to the vector $\mathbb{1}/N$. Figure S1 shows the TPMs before and after the update on $\sigma = 10$, where the colors represent the probabilities.

By adjusting different $alpha$, we can obtain the similar curves between Γ_α and EI as shown in Figure S2. We can observe that the positive correlations between EI and Γ_α can not be changed by different α , the shapes of the curves are different.

B.2 Softening of Controlled Degeneracy

The third model is very similar to the first one, however, the original matrix is not a permutation matrix, but a degenerated matrix. Here, a TPM is degenerative means that there are some row vectors are identical, and the number of identical row vectors is denoted as $N - r$ which is the controlled variable, where r is the rank of P . By tuning $N - r$, we can control the degeneracy [5] of the TPM as Figure S3 shows.

Without losing generality, we can start from an identity matrix, and change the controlled $N - r$ row vectors into the same one-hot vectors with all elements 0 except

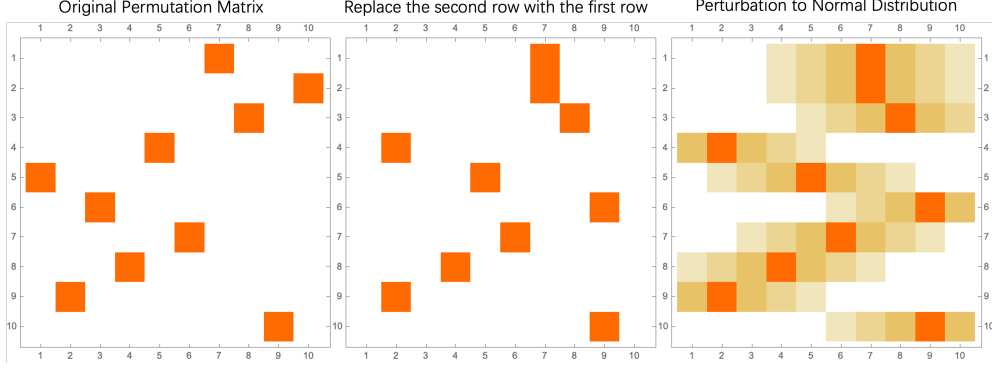


Fig. S3 The original TPM ($N = 10$), the replaced one to by controlling $N - r = 2$, and the perturbed TPM of the replaced one. Different colors represent different values of probability.

the last one is 1. After that, we soften the one hot vectors with the same method mentioned in Section B.1 to obtain the results in the main text and Figure 2(b).

B.3 Random Normalization

In this model, only two steps are required to generate a TPM: 1) Sample a row random vector from a uniform distribution in $[0, 1]$, 2) normalize this row vector such that the generated matrix is a TPM.

Appendix C Analytic solutions on the parameterized 2*2 TPM

We compare EI and Γ on a simplest example, the TPM is as:

$$P = \begin{pmatrix} p & 1-p \\ 1-q & q \end{pmatrix}, \quad (\text{C87})$$

where p and q are all free parameters in the range of $[0, 1]$. With this TPM, we can explicitly write down the expression for EI :

$$EI = \frac{1}{2} \left[p \log_2 \frac{2p}{1+p-q} + (1-p) \log_2 \frac{2(1-p)}{1-p+q} + (1-q) \log_2 \frac{2(1-q)}{1+p-q} + q \log_2 \frac{2q}{1-p+q} \right], \quad (\text{C88})$$

and Γ :

$$\Gamma = \sqrt{p^2 + (1-p)^2 + (1-q)^2 + q^2 + 2|1-q-p|}. \quad (\text{C89})$$

According these two expressions, we plot the landscapes in Figure 2(e) and (f).

Appendix D The coarse graining method based on SVD decomposition

We will first give the detailed introduction of the coarse-graining method based on SVD, and then we give an explanation why this simple method can work in practice.

D.1 The method

Intuitively, the basic idea of our method is to treat all row vectors P_i in P as data vectors with dimensionality of N , then we first take *PCA* dimensionality reduction for these row vectors, second to cluster them into r clusters where r is selected according to the threshold ϵ for singular value spectrum. With the clusters, we can reduce the original TPM according to the principle that all the stationary flows are conservative.

Concretely, the coarse-graining method contains five steps:

1) We first make SVD decomposition for P (suppose P is irreducible and recurrent such that stationary distribution exist):

$$P = U \cdot \Sigma \cdot V^T, \quad (\text{D90})$$

where, U and V are two orthogonal and normalized matrices with dimension $N \times N$, and $\Sigma = \text{diag}(\sigma_1, \sigma_2, \dots, \sigma_N)$ is a diagonal matrix which contains all the ordered singular values.

2) Selecting a threshold ϵ and the corresponding r if there is a clear cut off on the singular value spectrum;

3) Reducing the dimensionality of row vectors P_i in P from N to r by calculating the following Equation:

$$\tilde{P} \equiv P \cdot V_{N \times r}, \quad (\text{D91})$$

where $V_{N \times r} = (V_1^T, V_2^T, \dots, V_r^T)$.

4) Clustering all vectors in \tilde{P} into r groups by K-means algorithm to obtain a projection matrix Φ , which is defined as:

$$\Phi_{ij} = \begin{cases} 1 & \text{if } \tilde{P}_i \text{ is in the } r\text{th group} \\ 0 & \text{otherwise,} \end{cases} \quad (\text{D92})$$

for $\forall i, j \in [1, N]$.

5) Obtain the reduced TPM according to P and Φ .

To illustrate how we can obtain the reduced TPM, we will first define a matrix called stationary flow matrix as follows:

$$F_{ij} \equiv \mu_i \cdot P_{ij}, \forall i, j \in [1, N], \quad (\text{D93})$$

where μ is the stationary distribution of P which satisfies $P \cdot \mu = \mu$.

Secondly, we will derive the reduced flow matrix according to Φ and F :

$$F' = \Phi^T \cdot F \cdot \Phi, \quad (\text{D94})$$

where, F' is the reduced stationary flow matrix. The trade flow network in Figure 3(1) is obtained by F' and multiplying the total trade volume of each country. Finally, the reduced TPM can be derived directly by the following formula:

$$P'_i = F'_i / \sum_{j=1}^N (F'_i)_j, \forall i \in [1, N]. \quad (\text{D95})$$

Finally, P' is the coarse-grained TPM.

D.2 Explanation

We will explain why this coarse-graining strategy outlined in the previous sub-section works here.

In the first step, the reason why we SVD decompose the matrix P is that the singular values of P actually are the squared roots of the eigenvalues of $P^T \cdot P$ because:

$$P^T \cdot P = (P \cdot P^T)^T = (V \cdot \Sigma \cdot U^T) \cdot (U \cdot \Sigma \cdot V^T) = V \cdot \Sigma^2 \cdot V^T, \quad (\text{D96})$$

thus, we will try our best to utilize the corresponding eigenvectors in V to reduce P , because they may contain more important information of P .

Actually, the eigenvectors with the largest eigenvalues are the major axes to explain the auto-correlation matrix $P^T \cdot P$. Therefore we can use PCA method to reduce the dimensionality of $P_i, \forall i \in [1, N]$ s, it is equivalent to projecting P_i onto the subspace spanned by the r first eigenvectors.

In the fourth step, we cluster all the row vectors $P_i, \forall i \in [1, N]$ into $k < r$ groups according to the new feature vectors of P_i . Actually, according to the previous studies [33], these r major eigenvectors can be treated as the centroids of the clusters obtained by K-means algorithm for the row vectors $P_i, \forall i \in [1, N]$. Therefore, we cluster all row vectors in P by K-means algorithm, and the row vectors in one group should aggregate around the corresponding eigenvectors.

The final step is to obtain the reduced TPM according to the clustering result or Φ in the previous step. This is a classic problem of lumping a Markov chain [34, 35]. There are many lumping methods, and we adopt the one in [36].

The basic idea of this method is to keep the stationary distribution and the total stationary flux unchanged during lumping process because they can be understood as a conservative quantity such as energy flows or material flows. As a result, we derive the method mentioned in the previous sub-section.

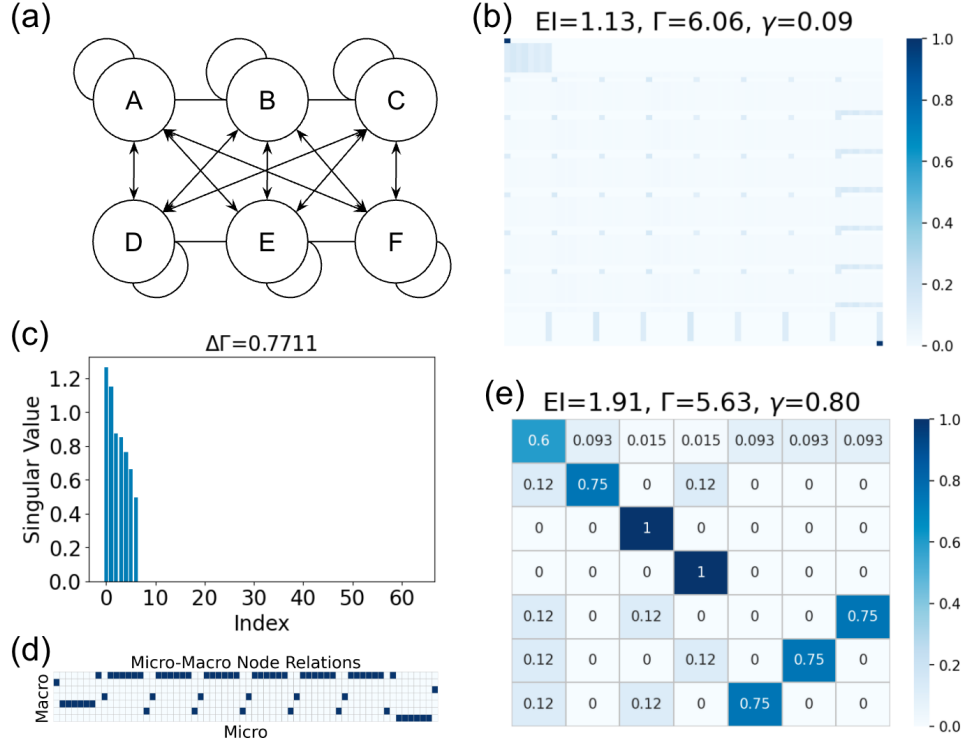


Fig. S4 (a) is a full-connection boolean network with two different types of edges. (b) is TPM reproduced from Fig.S2 of [5]. (c) is the singular spectrum of (b). (d) is projection matrix. (e) is coarse-grained TPM with our method. Here we get a larger macro EI than [5] (1.91 here and 1.84 in Hoel et al.'s work). It is because the macro TPM in [5] has 9 states, while our results only have 7. They treat $\{000111\}$ and $\{111000\}$ as two separate additional macro states as $\{02\}$ and $\{20\}$, while ours treats them as $\{11\}$.

Appendix E Applying our coarse-graining method on more examples

E.1 Examples of boolean networks in Hoel(2003)

To compare our method and EI maximization method, we apply our method to the examples of causal emergence in Hoel et al.'s original papers [5] and [6]. All the examples show clear causal emergence. And almost identical reduced TPMs are obtained for all the examples.

Figures S4 and S5 show additional examples from the SI, where our model predicts a higher macro EI compared to Hoel's findings. The main difference lies in our approach: Hoel groups variables to form a new macro network and then calculates EI for the TPM. We, on the other hand, group states directly, which might result in a TPM that doesn't fully represent the original Boolean network in terms of variables.

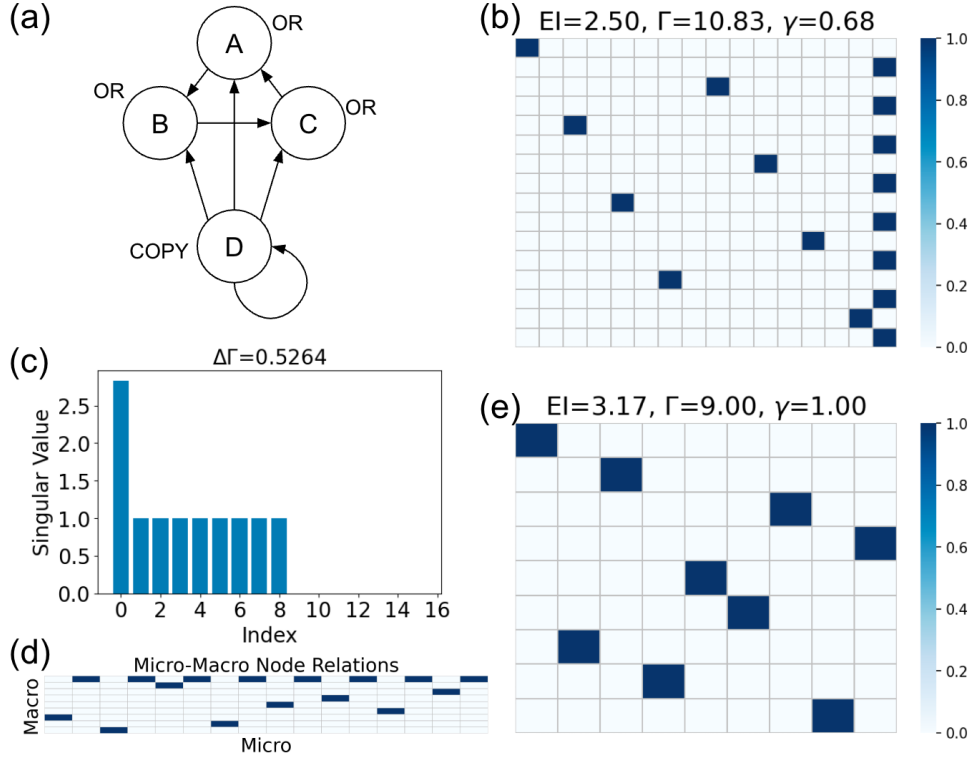


Fig. S5 (a) is a directed boolean network. (b) is the TPM of (a). (c) is the singular spectrum of (b). (d) is projection matrix. (e) is course-grained TPM. We also get a larger macro EI than Hoel's (3.17 here and 3.00 in [6]). It is because we have 9 macro states and [6] only has 8. We combined all the 8 micro states that transform to $\{11111111\}$ as a separate macro state, while [5] combines them into each of the other 8 groups.

Therefore, the extension of our method to variable-based coarse-graining method is deserve future studies.

References

- [1] Prigogine, I., Stengers, I.: The End of Certainty. Simon and Schuster, ??? (1997)
- [2] West, G.: Scale: The Universal Laws of Life, Growth, and Death in Organisms, Cities, and Companies. Penguin, ??? (2018)
- [3] Waldrop, M.M.: Complexity: The Emerging Science at the Edge of Order and Chaos. Simon and Schuster, ??? (1993)
- [4] Landau, L.D., Lifshitz, E.M.: Statistical Physics vol. 5. Elsevier, ??? (1980)
- [5] Hoel, E.P., Albantakis, L., Tononi, G.: Quantifying causal emergence shows that

- macro can beat micro. *Proceedings of the National Academy of Sciences of the United States of America* **110**(49), 19790–19795 (2013) <https://doi.org/10.1073/pnas.1314922110>
- [6] Hoel, E.P.: When the map is better than the territory. *Entropy* **19**(5) (2017) <https://doi.org/10.3390/e19050188>
- [7] Yuan, B., Zhang, J., Lyu, A., Wu, J., Wang, Z., Yang, M., Liu, K., Mou, M., Cui, P.: Emergence and causality in complex systems: A survey of causal emergence and related quantitative studies. *Entropy* **26**(2), 108 (2024)
- [8] Tononi, G., Sporns, O.: Measuring information integration. *BMC neuroscience* **4**, 1–20 (2003)
- [9] Zhang, J., Liu, K.: Neural Information Squeezer for Causal Emergence. *Entropy* **25**(1), 1–28 (2023) <https://doi.org/10.3390/e25010026> [2201.10154](https://arxiv.org/abs/2201.10154)
- [10] Mingzhe, Y., Zhipeng, W., Kaiwei, L., Yingqi, R., Bing, Y., Jiang, Z.: Finding Emergence in Data by Maximizing Effective Information
- [11] Rosas, F.E., Mediano, P.A., Jensen, H.J., Seth, A.K., Barrett, A.B., Carhart-Harris, R.L., Bor, D.: Reconciling emergences: An information-theoretic approach to identify causal emergence in multivariate data. *PLoS computational biology* **16**(12), 1008289 (2020)
- [12] Williams, P.L., Beer, R.D.: Nonnegative decomposition of multivariate information. *arXiv preprint arXiv:1004.2515* (2010)
- [13] Barnett, L., Seth, A.K.: Dynamical independence: discovering emergent macroscopic processes in complex dynamical systems. *Physical Review E* **108**(1), 014304 (2023)
- [14] Faye, J.: Causation, reversibility and the direction of time. In: *Perspectives on Time*, pp. 237–266. Springer, ??? (1997)
- [15] Bernardo, M., Lanese, I., Marin, A., Mezzina, C.A., Rossi, S., Sacerdoti Coen, C.: Causal reversibility implies time reversibility. In: *International Conference on Quantitative Evaluation of Systems*, pp. 270–287 (2023). Springer
- [16] Bernardo, M., Mezzina, C.A.: Bridging causal consistent and time reversibility: A stochastic process algebraic approach. *arXiv preprint arXiv:2205.01420* (2022)
- [17] Farr, M.: Causation and time reversal. *The British Journal for the Philosophy of Science* (2020)
- [18] Bernardo, M., Mezzina, C.A.: Bridging causal reversibility and time reversibility: A stochastic process algebraic approach. *Logical Methods in Computer Science* **19** (2023)

- [19] Kathpalia, A., Nagaraj, N.: Time-reversibility, causality and compression-complexity. *Entropy* **23**(3), 327 (2021)
- [20] Comolatti, R., Hoel, E.: Causal emergence is widespread across measures of causation. arXiv preprint arXiv:2202.01854 (2022)
- [21] Pearl, J., Mackenzie, D.: *The Book of Why: the New Science of Cause and Effect*. Basic books, ??? (2018)
- [22] Engleson, E., Azizpour, H.: Generalized jensen-shannon divergence loss for learning with noisy labels. *Advances in Neural Information Processing Systems* **34**, 30284–30297 (2021)
- [23] Stroock, D.W.: *An Introduction to Markov Processes* vol. 230. Springer, ??? (2013)
- [24] Schatten norm from Wikipedia. https://en.wikipedia.org/wiki/Schatten_norm
- [25] Recht, B., Fazel, M., Parrilo, P.A.: Guaranteed minimum-rank solutions of linear matrix equations via nuclear norm minimization. *SIAM review* **52**(3), 471–501 (2010)
- [26] Chi, Y., Lu, Y.M., Chen, Y.: Nonconvex optimization meets low-rank matrix factorization: An overview. *IEEE Transactions on Signal Processing* **67**(20), 5239–5269 (2019)
- [27] Cui, S., Wang, S., Zhuo, J., Li, L., Huang, Q., Tian, Q.: Towards discriminability and diversity: Batch nuclear-norm maximization under label insufficient situations. In: *Proceedings of the IEEE/CVF Conference on Computer Vision and Pattern Recognition*, pp. 3941–3950 (2020)
- [28] Fazel, M.: *Matrix rank minimization with applications*. PhD thesis, PhD thesis, Stanford University (2002)
- [29] Liu, L., Huang, W., Chen, D.-R.: Exact minimum rank approximation via Schatten p-norm minimization. *Journal of Computational and Applied Mathematics* **267**, 218–227 (2014)
- [30] Nie, F., Huang, H., Ding, C.: Low-rank matrix recovery via efficient Schatten p-norm minimization. In: *Proceedings of the AAAI Conference on Artificial Intelligence*, vol. 26, pp. 655–661 (2012)
- [31] Seabrook, E., Wiskott, L.: A tutorial on the spectral theory of markov chains. *Neural Computation* **35**(11), 1713–1796 (2023)
- [32] Matrix norm from Wikipedia. https://en.wikipedia.org/wiki/Matrix_norm

- [33] Ding, C., He, X.: K-means clustering via principal component analysis. In: Proceedings of the Twenty-first International Conference on Machine Learning, p. 29 (2004)
- [34] Marin, A., Rossi, S.: On the relations between lumpability and reversibility. In: 2014 IEEE 22nd International Symposium on Modelling, Analysis & Simulation of Computer and Telecommunication Systems, pp. 427–432 (2014). IEEE
- [35] Barreto, A.M., Fragoso, M.D.: Lumping the states of a finite markov chain through stochastic factorization. IFAC Proceedings Volumes **44**(1), 4206–4211 (2011)
- [36] Klein, B., Hoel, E.: The emergence of informative higher scales in complex networks. *Complexity* **2020**, 1–12 (2020)
- [37] Hoheisel, T., Paquette, E.: Uniqueness in nuclear norm minimization: Flatness of the nuclear norm sphere and simultaneous polarization. *Journal of Optimization Theory and Applications* **197**(1), 252–276 (2023)